

Faculté des lettres et sciences humaines  
Département de géomatique appliquée  
Université de Sherbrooke

## Comparisons of an aerosol transport model with a 4-year analysis of summer aerosol optical depth retrievals over the Canadian Arctic

« Comparaisons d'un modèle de transport d'aérosols avec une  
analyse de 4 ans de mesures estivales d'épaisseur optique  
d'aérosols dans l'Arctique canadien »

Sareh Hesaraki

Mémoire présenté pour l'obtention du grade de Maître en sciences  
géographiques (M. Sc.), cheminement télédétection

Septembre 2016

## **Composition du jury**

Ce mémoire a été évalué par un jury composé des personnes suivantes :

Prof. Norman T. O'Neill

Dép.de géomatique appliquée, Université de Sherbrooke

Directeur de recherche

Prof. Alain Royer

Dép.de géomatique appliquée, Université de Sherbrooke

Examineur

Prof. Martin Aubé

Dép. de physique, Cégep de Sherbrooke

Physics department of Bishop's University

Dép.de géomatique appliquée, Université de Sherbrooke

Examineur externe

# Abstract

This is a study concerning comparisons between the Dubovik Aerosol optical depth (AOD) retrievals from AEROCAN (ARONET) stations and AOD estimates from simulations provided by a chemical transport model (GEOS-Chem : Goddard Earth Observing System Chemistry). The AOD products associated with the Dubovik product are divided into total, fine and coarse mode components. The retrieval period is from January 2009 to January 2013 for 5 Arctic stations (Barrow, Alaska; Resolute Bay, Nunavut; OPAL and PEARL (Eureka), Nunavut; and Thule, Greenland). We also employed AOD retrievals from 10 other mid-latitude Canadian stations for comparisons with the Arctic stations.

The results of our investigation were submitted to Atmosphere-Ocean. To briefly summarize those results, the model generally but not always tended to underestimate the (monthly) averaged AOD and its components. We found that the subdivision into fine and coarse mode components could provide unique signatures of particular events (Asian dust) and that the means of characterizing the statistics (log-normal frequency distributions versus normal distributions) was an attribute that was common to both the retrievals and the model.

Keywords : Aerosol, Aerosol Optical Depth (AOD), GEOS-Chem, AEROCAN, Dubovik inversion

# Résumé

Cette étude compare des épaisseurs optiques d'aérosols (AOD) à 5 stations arctiques d'AEROCAN (AERONET), obtenues d'une part à l'aide de l'algorithme d'inversion de Dubovik appliqué à des mesures in situ, et d'autre part du modèle de transport chimique (GEOS-Chem : Goddard Earth Observing Système Chemistry). Les produits d'AOD associés à l'algorithme d'inversion sont divisés en composantes totales, fines et grossières. Pour chacune des 5 stations (Barrow, Alaska, Resolute Bay, au Nunavut, OPAL et PEARL (Eureka), Nunavut, et Thulé, au Groenland), la période de récupération est de janvier 2009 à janvier 2013. Nous avons également utilisé les mesureurs d'AOD de dix autres stations canadiennes de latitudes moyennes, à des fins de comparaison.

Les résultats de l'étude ont été soumis à la revue *Atmosphere-Ocean*. Pour résumer brièvement ces résultats, le modèle a généralement, mais pas toujours, eu tendance à sous-estimer l'AOD moyenne et de ses composantes. Nous avons constaté que la subdivision en composantes fine et grossière pourrait fournir des signatures uniques d'événements particuliers (poussière asiatique) et que les moyens de caractériser des statistiques (les distributions de fréquence log-normale versus les distributions normales) était un attribut qui était commun aux deux les mesureurs et le modèle.

Mots clés : Aérosol, épaisseur optique d'aérosol, GEOS-Chem, AEROCAN, inversion Dubovik

# Table of Contents

<b>Abstract</b> .....	<b>i</b>
<b>Résumé</b> .....	<b>ii</b>
<b>List of Figures</b> .....	<b>v</b>
<b>List of Tables</b> .....	<b>vi</b>
<b>Preface</b> .....	<b>vii</b>
<b>Acknowledgements</b> .....	<b>viii</b>
<b>CHAPTER 1. General introduction</b> .....	<b>1</b>
1.1 Atmospheric aerosols.....	1
1.2 Different types of aerosols and their sources.....	2
1.3 Aerosol spatio-temporal simulation using chemical transport models .....	2
1.4 Objectives and hypothesis of the mémoire .....	3
1.5 Overview of the article submitted as part of this mémoire .....	3
<b>CHAPTER 2. Comparisons of an aerosol transport model with the analysis of aerosol optical depth retrievals over the Canadian Arctic</b> .....	<b>5</b>
2.1. Introduction.....	7
2.2. Background.....	9
2.2.1 Sun photometry and sky radiometry .....	9
2.2.2 Averaging and standard deviation statistics.....	9
– Averaging nomenclature.....	9
– Averaging procedure and the interpretation of successive averaging.....	10
– Lognormal versus normal representations .....	11
2.3. Methodology.....	12
2.3.1 AEROCAN / AERONET sites employed in this study .....	12
2.3.2 Ground-based retrievals of AOD .....	14
2.3.3 Level 1.5 versus Level 2.0 retrievals .....	16
2.3.4 GEOS-Chem simulations.....	17
2.3.5 AOD differences due to small changes in the reference wavelength: GC versus AERONET retrievals.....	18
2.4. Results and discussions for the Canadian Arctic.....	19

2.4.1	Analysis of lognormal versus normal representations .....	19
2.4.2	General AOD statistics for the retrievals .....	21
–	General considerations .....	21
–	Seasonal variations of the total AOD .....	24
2.4.3	Comparisons with GC .....	25
–	Component AODs averaged over all stations .....	25
–	Individual stations .....	27
2.5.	Conclusions .....	34
2.6.	References of the paper .....	36
	Symbol and acronym glossary .....	40
	<b>CHAPTER 3. Conclusions and recommendations .....</b>	<b>41</b>
	<b>Appendix A .....</b>	<b>43</b>
	Correlation between measurements & model .....	43
	<b>Appendix B .....</b>	<b>46</b>
	Intra-annual AODs versus time .....	46
	<b>References .....</b>	<b>48</b>

# List of Figures

Figure 1. Map showing the five Arctic stations whose data was used in this study as well as the 10 southern stations whose data was employed for purposes of comparison with the Arctic data. .... 13

Figure 2. Normal and log-normal fit comparisons for AERONET and GC AOD histograms (a) Linear and lognormal histograms (left and right-hand graphs, respectively) for AERONET at  $\lambda = 500$  nm and GC at  $\lambda = 550$  nm (top and bottom rows respectively), (b) An example of how to employ the traditional means of reporting sun photometry AOD statistics (linear mean and standard deviation) to extract parameters that are representative of the lognormal distribution. In this illustration the linear mean and standard deviation are used to estimate the geometric mean of the histogram by calculating the latter from the lognormal parameterization (equations (2) and (3))..... 20

Figure 3. Comparison between various types of monthly averages (black and purple) and the monthly averages (green) of Tomasi et al. (2015). The Tomasi AOD averages represent Level 2.0 extinction data. The purple curve shows the averages for the MYSP. The error bars are standard deviations..... 23

Figure 4.  $\langle \tau_a \rangle$  (averaged over the 2009 to 2112 MYSP) as a function of month for the Arctic stations compared with the analogous averages for the 10 southern stations. The error bars are standard deviations..... 25

Figure 5.  $\langle \tau_f \rangle$ ,  $\langle \tau_c \rangle$  and  $\langle \tau_a \rangle$  (monthly averages over the 2009 to 2112 MYSP) and modelled values ( $\langle \tau_f, GC \rangle$ ,  $\langle \tau_c, GC \rangle$  and  $\langle \tau_a, GC \rangle$ ) as a function of month. The error bars are standard deviations. .... 26

Figure 6. Coefficient of determination between modelled and retrieved daily AOD means for the ensemble of all sites ("all") and for individual sites. The error bars are the standard deviations corresponding to one standard deviation of Fisher's z transformation distribution (see Siegel, 1961, for example). .... 28

Figure 7.  $\langle \tau_f \rangle$  Fine mode monthly averages over the MYSP for all 5 Arctic sites. The error bars are the standard deviations. .... 30

Figure 8.  $\langle \tau_c \rangle$  Coarse mode monthly averages over the MYSP for all 5 Arctic sites. The error bars are the standard deviations. .... 32

Figure 9. Scattergrams in log-log space of the model versus AERONET retrievals (a for fine mode, b for coarse mode and c for total AOD) based on a linear regression (bold line) and logarithmic regression (thicker dashed line) for the ensemble of all sites. The very short dashed line is the  $y=x$  line. .... 45

Figure 10. Intra-annual variation of fine AODs over the MYSP..... 46

Figure 11. Intra-annual variation of coarse AODs over the MYSP..... 47

# List of Tables

Table 1. AEROCAN/AERONET sites employed in this study.....	14
Table 2. Ensemble monthly means of Level 1.5 and Level 2.0 AOD components and the differences of two levels for 5 Arctic stations over the period of 2009-2012. ....	17



# Preface

This document presents the results of a Master's thesis carried out at l'Université de Sherbrooke at the Department of Applied Geomatics under the supervision of Professor Norm O'Neill.

This thesis is based on an article entitled 'Polar summer comparisons of a chemical transport model with a 4-year analysis of fine and coarse mode aerosol optical depth retrievals over the Canadian Arctic' that was submitted to a peer reviewed journal, Atmosphere-Ocean on August.29, 2016. Sareh Hesaraki is the first author with Norman T. O'Neill, Glen Lesins, Auromeet Saha, Randall V. Martin, Vitali E. Fioletov, Konstantin Baibakov, and Ihab Abboud being the co-authors.

# Acknowledgements

My deepest gratitude is to my director, Professor Norm O'Neill. I have been amazingly fortunate to have an advisor who gave me the freedom to explore on my own and at the same time the guidance to recover when my steps faltered.

I am also indebted to Professor Glen Lesins as well as Professor Randall Martin and his research group at Dalhousie University : this work would not have been possible without their help.

I would like to acknowledge the principal investigators of the AERONET sites whose data I used in my Master's project.

The results of this study are part of a larger NSERC – CCAR (National Sciences and Engineering Research Council - Climate Change and Atmospheric Research) funded project called NETCARE (NETwork on Climate and Aerosols : addressing key uncertainties in Remote Canadian Environments).

# CHAPTER 1. General introduction

## 1.1 Atmospheric aerosols

Atmospheric aerosols are small particles whose size (radius) varies from  $\sim 0.001 \mu\text{m}$  to  $100 \mu\text{m}$  and which are in solid, liquid or mixed phase (see Hinds, 1998 for fundamental text on the nature of aerosols and their measurement). These particles have impacts on human health inasmuch as they are commonly associated with pollution as well as important impacts on climate change. According to the authors of the IPCC, working group I report, aerosols represent the largest uncertainty in radiative forcing calculations (IPCC, 2013). This uncertainty manifests itself as the uncertainty in describing the direct and indirect effect of aerosols. The former effect, which is largely a cooling phenomenon, results from aerosol backscattering of solar radiation into space. The latter effect is the consequence of aerosols acting as condensation or ice forming nuclei for cloud particles and the fact that the properties of those cloud particles are dependent on the properties of the aerosol nuclei.

The aerosol parameters considered in this study, are of two different types (see the introduction section of the submitted paper in the next chapter for more details). These parameters can be extensive in nature inasmuch as they vary with the number (amount) of aerosols : typically such properties are rather localized in space and time and are subject to high frequency variations in both those dimensions. Alternatively, they can be intensive in nature (per particle properties) : intensive properties tend to be more regional in space inasmuch as they are associated with the type (source) of the aerosol or hence with the type of air mass. The most important extensive parameter in our research is AOD (Aerosol Optical Depth) while the important intensive aerosol parameters are particle size and particle nature (nature being represented by refractive index in an optical sense and composition in a microphysical sense).

The research carried out for this thesis was associated with a sub-project of NETCARE (Abbatt, 2012). NETCARE is a collaborative project involving academic participants from a number of Canadian universities as well as government participants from Environment Canada (EC) and The Department of Fisheries and Oceans Canada (DFO).

## **1.2 Different types of aerosols and their sources**

According to Hinds (1998), aerosols can be divided into different size categories: nucleation mode (0.001  $\mu\text{m}$  – 0.01 $\mu\text{m}$  radius), Aitken mode (0.01 $\mu\text{m}$  – 0.1 $\mu\text{m}$ ), accumulation mode (0.1 $\mu\text{m}$  - 1 $\mu\text{m}$ ) and coarse mode (>1 $\mu\text{m}$ ). Aerosols come from natural and anthropogenic sources. In terms of significant optical effects in the visible and near infra-red region these four modes essentially reduce to the accumulation (fine) mode and the coarse mode (O'Neill et al., 2001). Natural aerosols have diverse origins, including, for example volcanic eruptions, wild fires, wind impacted mineral dust over deserts, and sea salt from sea spray. Anthropogenic aerosols such as sulphates, nitrates and carbonaceous aerosols come mainly from combustion processes (Jacob, 1999).

Both natural and anthropogenic aerosols can be grouped into two categories : primary and secondary aerosols. Primary aerosols are mostly coarse mode particles emitted directly into the atmosphere by disintegration and / or dispersion of plant, and animal matter (or the microbes from different living or non-living surfaces). Fine mode secondary aerosols, however, begin as gases which subsequently form aerosols after gas to particle conversion processes (see Seinfeld & Pandis, 2006 for a general reference on aerosol types). In general, the subdivision into fine and coarse mode components is important for understanding the dynamics of aerosols since the separate modes generally represent independent types of aerosols

## **1.3 Aerosol spatio-temporal simulation using chemical transport models**

Concentrations of aerosol (and other atmospheric constituents) can be estimated from models without, in the first instance, the direct use of observations. Chemical Transport Models (CTMs) simulate the temporal and spatial evolution of aerosol and gaseous compounds using meteorological data sets, emission inventories, as well as the physical and chemical laws that govern the behaviour of atmospheric constituents (Van Donkelaar et al., 2012). GEOS-Chem (the global CTM that we employed in our paper) has proven to be useful in analyzing atmospheric observations and to achieve a better understanding of aerosol dynamics on global and regional scales. The NETCARE strategy, with respect to the GEOS-Chem model, is to test various approaches and algorithms, and subsequently

recommend mature algorithms to be implemented in the models that simulate aerosol dynamics across the Canadian domain (Abbatt, 2012).

#### **1.4 Objectives and hypothesis of the mémoire**

Model simulations are widely used to achieve a more universal understanding of the dynamics of aerosols and their impact on climate change and air quality (Martin et al., 2010). These simulations involve complex inputs, processes, scaling considerations, etc. that, at one level or another must be compromised by the limitations of available computational resources as well as the limitations in our understanding of the basic mechanisms that influence the spatio-temporal evolution of aerosol properties. They therefore must be compared with aerosol measurements and adapted to the reality defined by those measurements. The information obtained from local, regional or global scale remote sensing of aerosols is arguably the most important model comparison source for measurements of aerosol models.

The present work falls within Activity 4 of the NETCARE program ("Implications of Measurements on Simulations of Atmospheric Processes and Climate."). Verifying the aerosol predictive capabilities of the GEOS-Chem model in comparisons with AERONET/AEROCAN retrievals of total, fine and coarse mode AODs was our objective within the larger context of Activity 4).

The GEOS-Chem capability of predicting the important (and robust) aerosol optical parameter of AOD, within the error uncertainty of the measurements, is the basis of the hypothesis that we sought to validate within the context of this study. Realistically we hoped to employ monthly means and the associated (natural) standard deviation of the measurements and the models as significance constraints on the intercomparability of total, fine and coarse mode AODs (where total AOD is simply the sum of the fine and coarse mode AODs).

#### **1.5 Overview of the article submitted as part of this mémoire**

The climate behaviour of aerosols and their pollution effects in high latitude regions like the Arctic are not well known. Understanding the behaviour of aerosols in remote regions is important for modellers who wish to adequately characterize the meteorological scale

pollution impacts of aerosols as well as the longer term climate impacts in a region where such impacts are known to be magnified (IPCC technical summary of working group 2). The article that follows (Chapter 2) addresses certain elements of NETCARE Activity 4 ("Implications of measurements on simulations of atmospheric processes and climate" as defined in Abbatt, 2012). Future modifications of the paper during the revisions phase of the journal review will take into account some points to improve that were noted by the members of the mémoire jury.

The principal objective of the paper is to compare the polar summer simulations of a chemical transport model (GEOS-Chem) with a climatology of total, fine and coarse mode AOD retrievals over five Canadian Arctic stations. These retrievals depend on measurements of spectral AOD and sky radiance acquired by CIMEL instruments of the AEROCAN / AERONET network and the fundamental concept that much of aerosol optical behaviour can be understood in terms of fine / coarse bimodal size distributions (O'Neill et al., 2001). Comparisons with the model exploit its ability to subdivide aerosol types into fine and coarse mode components and, in turn, their fine and coarse mode AODs. The most important contribution of the paper relates to the fact that the coarse mode retrievals, even though their relative errors are very large, are a fairly unique indicator of what is likely Asian dust because (a) the timing is right (April), (b) GEOS-Chem says the same thing (and says that the coarse mode AODs are dominated by dust), (c) the separation into fine and coarse mode allows a very weak signal ( $\tau_c$  from the retrievals  $\sim 0.01$ ) to be discriminated from the background in spite of the fact the expected errors of the retrieval method (something bigger than the typical CIMEL AOD errors of 0.01 to 0.02) are competitive if not larger than the nominal  $\tau_c$  values, (d) that GEOS-Chem coarse mode AODs are significantly correlated with coarse mode retrievals (the correlations were marginal for total AODs, so division into coarse and fine modes was a significant step), (e) that people generally don't think of this nuanced means of verifying a model and that there is little in the literature related to an evaluation of that nature that we are aware of. It was also demonstrated that both the measurements and the model were characterized by frequency distributions that were lognormal and that this characteristic led to better model vs retrieval correlations in log-log space.

## CHAPTER 2. Comparisons of an aerosol transport model with the analysis of aerosol optical depth retrievals over the Canadian Arctic

Paper title:

Polar summer comparisons of a chemical transport model with a 4-year analysis of fine and coarse mode aerosol optical depth retrievals over the Canadian Arctic

(Les comparaisons d'été polaires d'un modèle de transport chimique avec une analyse de 4 ans des mesureurs d'épaisseur optique des aérosols en composantes fines et grossières dans l'Arctique canadien)

Paper submitted to the journal of Atmosphere-Ocean on August 29, 2016

Sareh Hesaraki<sup>1\*</sup>, Norman T. O'Neill<sup>1</sup>, Glen Lesins<sup>2</sup>, Auromeet Saha<sup>1</sup>, Randall V. Martin<sup>2,3</sup>, Vitali E. Fioletov<sup>4</sup>, Konstantin Baibakov<sup>5</sup>, Ihab Abboud<sup>4</sup>

1. Centre d'Applications et de Recherches en Télédétection, Université de Sherbrooke, Sherbrooke, QC, Canada.
2. Department of Physics and Atmospheric Science, Dalhousie University, Halifax, N.S. Canada.
3. Also at Harvard-Smithsonian Center for Astrophysics, Cambridge, Massachusetts, United States.
4. Environment and Climate Change Canada (ECCC), Toronto, ON, Canada.
5. National Research Council Canada, Flight Research Laboratory, Ottawa, Canada.

## **Abstract**

We compared AERONET retrievals of total, fine-mode (sub-micron), and coarse-mode (super-micron) aerosol optical depth (AOD) with simulations from a chemical transport model (GEOS-Chem) across five Arctic stations and a four year, Polar summer, sampling period. It was determined that the AOD histograms of both the retrievals and the simulations were better represented by a lognormal distribution and that the successful simulation of this empirical feature as well as its consequences (including a better model versus retrieval coefficient of determination in log-log AOD space) represented a general indicator of model evaluation success. Seasonal (monthly averaged) AOD retrievals were sensitive to how the averaging was performed: this was ascribed to the presence of highly variable fine mode smoke. The retrieved and modelled station-by-station fine mode AOD averages showed a peak in April / May which decreased across the summer period while the model underestimated the fine mode AOD by an average of about 0.01. Both the retrievals and simulations showed seasonal coarse mode AOD variations with a peak in April / May that was attributed to Asian dust. The success in capturing such weak seasonal events helps to confirm the relevance of the fine / coarse mode separation and the validity of model estimates in the Arctic.

Keywords: AERONET, Aerosol Optical Depth, Arctic, Chemical Transport Model, GEOS-Chem



## 2.1. Introduction

The IPCC (2013) affirmation concerning the importance of understanding aerosol contributions to the direct and indirect effect is of particular significance over the Arctic where climate change impacts are known to be magnified. In order to properly analyse aerosol processes and emission modelling in chemical transport models (CTMs) one needs to develop a reliable and varied measurement program to exercise as many of the aerosol functionalities as possible. Ground-based sun photometry measurements of aerosol optical depth (AOD) and sky radiance measurements represent key components of such a measuring program since they provide vertically averaged, robust parameters that define the macroscale, 1st order comparative constraints that models must satisfactorily simulate.

A climatological-scale analysis of AOD and its derivative products represents a basis of model comparison that gives perspective to more spatially and temporally demanding (event scale) comparisons. Such analyses can permit one to effectively filter out information about the most robust and fundamental mechanisms that control aerosol behaviour. Also, the AOD contamination impact of clouds and other sources of sun photometry error as well as the AOD computation impact of model limitations such as spatial resolution and time-step resolution are often dampened by carrying out comparisons at climatological scales.

The aerosol optical properties derived from sun photometry are predominantly constrained by a simple concept of bimodality : the detectable optical effects are largely driven by a bimodal (volume) particle size distribution (PSD) consisting of a fine mode or submicron component and a coarse mode or super micron component (see, for example, Whitby et al., 1972 for an earlier statement on the microphysical bimodality of the volume PSD and O'Neill et al., 2001 for a discussion of the optical bimodality). This concept represents a higher order but (still) robust approach relative to the classical Angstrom approximation for which the aerosol model is a simple, monotonically decreasing PSD (a Junge distribution for which the volume PSD, varying as  $r^{-\alpha}$  yields an AOD spectrum that varies as  $\lambda^{-\alpha}$  :  $\alpha$  being the classical Angstrom exponent determined from a multi-band,  $\log(\text{AOD})$  versus  $\log(\lambda)$  regression)).

The bimodality concept means that one can divide aerosol optics into total, fine and coarse mode AODs, Angstrom exponents and their derivative ( $\tau_a$ ,  $\alpha$ ,  $\alpha'$ ;  $\tau_f$ ,  $\alpha_f$ ,  $\alpha_f'$ ;  $\tau_c$ ,  $\alpha_c$ , and  $\alpha_c'$  respectively, c.f. O'Neill et al., 2001). This presents an alternative, and arguably more natural means, of evaluating columnar CTM outputs whose microphysics packages are (appropriately) based on fine and coarse mode aerosol species. Bi-modality represents a purer apportionment into extensive (quantity dependant) and intensive (per particle) optical properties ( $\tau_a$ ,  $\tau_f$ ,  $\tau_c$  and  $\alpha$ ,  $\alpha_f$ ,  $\alpha_c$ , etc respectively).

Model evaluation and comparison in the literature is largely based on comparisons of AOD and  $\alpha$  as well as speciated surface concentrations. In the Arctic, Hardenberg et al., (2012) compared AODs and regression Angstrom exponents simulated by two global models (ECHAM-HAM and TM5) with AODs extracted from the Polar AOD network & MODIS data over 6 Arctic stations for a sampling period extending from 2001 to 2006. They found that the models reproduced good estimates of Angstrom exponent but significantly underestimated the measured AODs. Breider et al. (2014) compared seasonal GEOS-Chem estimations of Arctic AOD with AODs measured at 8 Arctic stations for a sampling period of 1999 -2011. They observed that the model had succeeded in simulating AERONET AODs and provided model-based, speciation insight into how the constituent components would have contributed to the total AOD (including a general apportionment into natural and anthropogenic aerosols). Shindell et al. (2008) and Eckhardt et al. (2015) carried out multi-model comparisons with surface aerosol concentrations measured in the Arctic. A notable feature of Shindell's comparisons was the large amount of variation in seasonal concentration between the estimates of different models (attributed to differences in aerosol and chemical physical processing, including removal). Eckhardt et al. (2015) noted large model variation (for sulfates) over the Arctic and observed that the models appeared to capture BC and sulfate concentrations while struggling to capture the extremes of the seasonal variation of the surface concentrations (notably the higher concentrations of the Arctic Haze in the springtime and the lower concentrations characteristic of the summertime).

In this paper we performed seasonal (monthly resolution) comparisons between the species dependent AODs simulated by a community CTM (GEOS-Chem) and AERONET sun photometry / radiometry retrievals of total, fine and coarse mode optical

depths over sites in or near the Canadian Arctic. The comparisons were carried out across a multi-year sampling period (MYSP) of 4 years (2009 – 2012). One of our major goals was to demonstrate the advantages of such an approach within a context of more traditional comparisons with generic AODs and Angstrom exponents. The investigation also includes an analysis of the most relevant means of presenting statistical results for both retrievals and simulations.

## 2.2. Background

### 2.2.1 Sun photometry and sky radiometry

The sun photometry / sky radiometry capabilities of the AERONET network provide classical measurements of spectral AOD in the solar extinction mode and angular measurements of sky radiance in the almucantar mode (Holben et al., 2001). The spectral AOD mode provides robust microphysical and / or optical retrievals with limited degrees of freedom while the combination of spectral AOD and sky radiance measurements provides microphysical and/or optical retrievals of multiple degrees of freedom (see Twomey & Howell, 1967 for a general discussion on, respectively, the number of degrees of freedom in "transmission" and "forward scattering" mode). In the extinction mode one can employ an algorithm such as the (Spectral Deconvolution Algorithm) SDA (O'Neill et al., 2003) to extract  $\tau_a$ ,  $\tau_f$ , and  $\tau_c$  at a reference wavelength of 500 nm (the AERONET standard). In extinction / sky radiance mode one can extract particle size distribution and refractive index (Dubovik et al., 2000) and employ these results to compute 4-channel spectra of  $\tau_a$ ,  $\tau_f$ ,  $\tau_c$  which can be interpolated to a reference wavelength such as 500 nm. The two sets of quantities are very similar but the SDA represents a spectral retrieval approach while the Dubovik retrieval literally divides the retrieved particle size distribution at a specific radius (c.f. O'Neill et al., 2003).

### 2.2.2 Averaging and standard deviation statistics

#### – Averaging nomenclature

In general, we will let  $\langle \tau_x \rangle$  and  $\sigma_x$  represent the arithmetic average and standard deviation across any averaging bin. These statistical parameters clearly depend on

conditions such as site, year, etc. Rather than overload the nomenclature with more subscripts, we will explain the context depending on the case being considered. Similarly, we will represent the geometric mean and standard deviation (that result from averages and standard deviations of  $\log(\tau_x)$ ) by  $\tau_{g,x}$  and  $\mu_x$ . In the following section we discuss some implications of the averaging scheme (for this particular section only, we used a more elaborate subscribing scheme to help clarify the details of successive averaging).

– Averaging procedure and the interpretation of successive averaging

At any statistical level in this work we calculated an average or a standard deviation by employing all individual retrievals in any "averaging bin" (days, months, years, stations etc.). While one can debate the merits of any given averaging approach (see Levy et al., 2009, for example), the approach of employing individual measurements does have the distinct advantage of providing a clear point of reference for the averaging chain. Given this statistical protocol, it behoves one to be clear on how the relationship between successive averages across different averaging bins can be interpreted (simply because it is an inevitable question which arises as one statistically processes the data).

It is easy to demonstrate that requiring averages that employ all original measurements for a given averaging bin equates to a higher level average (monthly average, for example) being the weighted average of lower level averages (daily averages, for example) where the weights are the normalized number of measurements that contributed to the lower level averages (normalized number of measurements per day for our particular example). Thus the monthly AOD average of daily averages across month "k" would be:

$$\tau_{x,k} = \sum_{j=1}^{J_k} \omega_{k,j} \tau_{x,k,j} \quad \text{where} \quad \omega_{k,j} = \frac{N_{k,j}}{N_k} \quad (1)$$

where  $\tau_{x,k,j}$  and  $N_{k,j}$  represent respectively the measurement and the number of measurements acquired on day "j" of month "k" and  $N_k$  is the total number of measurements during month "k" (we could have also proceeded by considering the means of  $\log(\tau_{x,k})$  as per the section below on lognormal distributions). An analogous relation

would be then employed to proceed up another level of successive averaging (which could be, for example, averaging across all stations for a given month "k"). It is also easy to show that the average obtained for a given set of averaging bins is independent of the order of the averaging (for example, monthly averages for a given year and station to yearly averages for a given station to station averages across the total ensemble (total MYSP data set) of retrievals can be performed as monthly averages to station averages to yearly averages and the result would be the same). This commutativity property applies only to the measurement-frequency weighting scheme as defined in equation (1) and not the general-purpose type of weighting schemes discussed in Levy et al. (2009).

– Lognormal versus normal representations

Various investigations in the literature have led to the observation that AOD histograms are better represented by a lognormal distribution as opposed to a normal distribution (which means that the AOD histogram is more realistically represented by a normal or Gaussian curve in logarithmic space and a long-tailed, positively skewed curve in linear space). These investigations include those of O'Neill et al. (2000), Knobelspiesse et al. (2004) and Perrone et al. (2005) for sun photometric data, Matthias et al. (2004) for lidar-retrieved AODs and Ignatov and Stowe (2002) for satellite-retrieved AODs. In terms of Arctic AOD multi-year analyses, the long-tailed, positively skewed asymmetry typical of a lognormal distribution appears in the histograms of Tomasi et al. (2015). In spite of this evidence for lognormality, the persistent if understandable inertia of historical reporting means that the AOD community, including some, if not all, of the co-authors of this paper, continue to report arithmetic statistics rather than geometric statistics. Basically this amounts, respectively, to reporting AOD statistics as the arithmetic mean and standard deviation<sup>1</sup>  $\langle \tau_x \rangle \pm \sigma(\tau_x)$  rather than as the geometric mean and standard deviation,  $\tau_{x,g} \times \mu_x^{\pm 1}$  (or some related form depending on the desired probability metric). The latter expression is almost invariably a better representation of the AOD histogram (as well as derived parameters such as the median and peak values). This fact has non-trivial consequences: a climate modeller, for example, who wanted to report the

---

<sup>1</sup> See the acronym glossary where the means and standard deviation parameters are defined (x = a, f, or c).

most probable AOD of a future AOD distribution would be distinctly incorrect in tying the objective analysis to an assumption that  $\langle \tau_x \rangle$  was the most probable value.

The inertia of traditional reporting protocols aside, the geometric mean and standard deviation approach is rarely used because people are generally not as comfortable with logarithmic statistics as they are with linear statistics (and / or because they are not aware of the simple formulation above). In any event, the more relevant geometric statistics can be retrieved from the arithmetic statistics. It is easy to show (from Table 1 of O'Neill et al., 2000) that the former can be related to the latter:

$$\tau_{g,x} = \langle \tau_x \rangle \exp(-\ln^2(\mu_x/2)) \quad \text{where,} \quad (2)$$

$$\mu_x = \exp \left[ \sqrt{\ln \left( 1 + \left( \frac{\sigma(\tau_x)}{\langle \tau_x \rangle} \right)^2 \right)} \right] \quad (3)$$

Limpert et al. (2001) make essentially the same argument (on the reporting of arithmetic statistics for data distributions that are clearly lognormal) in their general treatise on lognormal distributions in the sciences.

The arithmetic and geometric statistics of measured and GC-simulated AODs will be compared below. Within the context of the model comparison goals of this paper, we seek to demonstrate that GC AODs generally subscribe to the same lognormal properties as retrieved AODs.

## 2.3. Methodology

### 2.3.1 AEROCAN / AERONET sites employed in this study

Figure 1 shows the AEROCAN / AERONET sites which were employed for our GC comparisons (AEROCAN is the Canadian federated subnetwork of AERONET) while Table 1 gives the location and instrumental details for all sites.

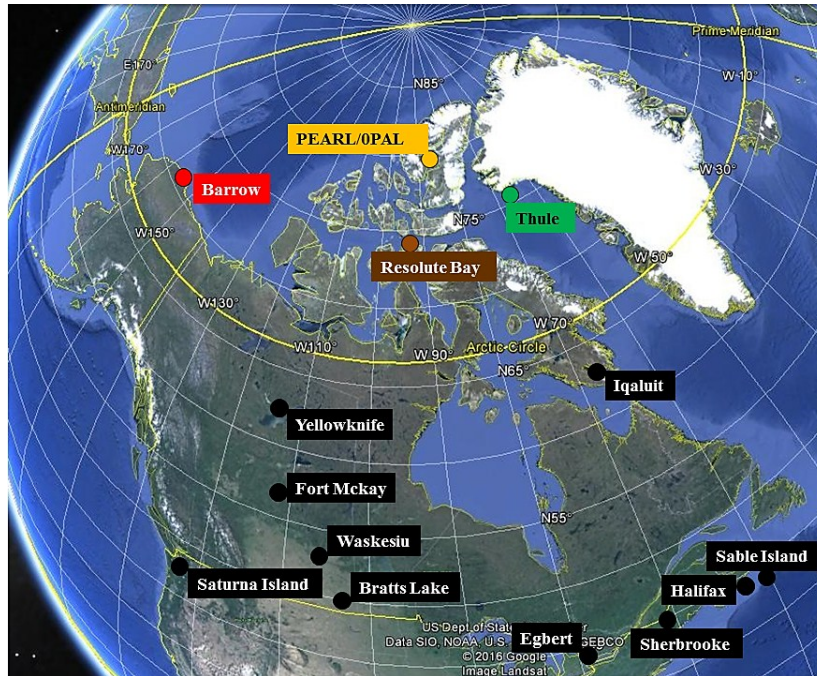


Figure 1. Map showing the five Arctic stations whose data was used in this study as well as the 10 southern stations whose data was employed for purposes of comparison with the Arctic data.

Our study was focussed on three sites in the Canadian Arctic (the 0PAL, PEARL AEROCAN sites at Eureka and Resolute Bay) and two other Arctic AERONET sites at the boundaries of the Canadian Arctic (Barrow, AK and Thule, Greenland). 0PAL and PEARL are located at Eureka, Nunavut with the 0PAL site being at a near sea-level elevation while the PEARL site is on a ridge about 15 km away at an elevation of 610 meters. These two sites provide a degree of data redundancy which we often exploit to verify the robustness of retrievals. A series of 9 southern Canadian AEROCAN sites were employed to present comparative statistics with the Arctic retrievals.

Table 1. AEROCAN/AERONET sites employed in this study.

	Latitude (°N)	Longitude (°W)	Elevation (meters)	Data acquisition period
<b>Arctic</b>				
Barrow, AK, USA <sup>2</sup>	71° 18' 43"	156° 39' 54"	0	2001-2012
OPAL, Eureka, NV <sup>3</sup>	79° 59' 24"	85° 56' 20"	0	2007-2012
PEARL, Eureka, NV	80° 03' 14"	86° 25' 01"	615	2007-2011
Resolute Bay, NV <sup>3</sup>	74° 43' 58"	94° 54' 00"	40	2004-2012
Thule, Greenland <sup>2</sup>	76° 30' 57"	68° 46' 08"	225	2007-2012
<b>Southern sites</b>				
Bratt's Lake, SK <sup>4a</sup>	50° 16' 48"	104° 42' 00"	586	2004-2012
Saturna Island, BC <sup>4b</sup>	48° 46' 58"	123° 07' 58"	200	2004-2012
FortMckay, AB <sup>4c</sup>	57° 11' 02"	111° 38' 24"	267	2004-2012
Yellowknife, NWT <sup>4d</sup>	62° 27' 07"	114° 24' 25"	201	2008-2012
Waskesiu, SK	53° 55' 01"	106° 04' 58"	550	2005-2012
Iqaluit, NV <sup>3</sup>	63° 44' 52"	68° 32' 34"	15	2008-2010
Egbert, ON <sup>4e</sup>	44° 13' 33"	79° 45' 00"	264	2004-2012
CARTEL, Sherbrooke, QC <sup>4f</sup>	45° 22' 44"	71° 55' 51"	300	2004-2012
Halifax, NS <sup>4g</sup>	44° 38' 16"	63° 35' 38"	65	2004-2012
Sable Island, NS	43° 55' 58"	60° 00' 36"	3	2010-2012
<b>Notes</b>				
1. Sites have a nominal AOD sampling rate of 3 minutes (except for Barrow whose nominal rate is 15 minutes)				
2. AERONET sites that are close to the AEROCAN regions				
3. Nunavut, Canada. There was no data in 2005				
4. "a" to "g"; the Canadian provinces of Saskatchewan, British Columbia, Alberta, North West Territories, Ontario, Québec, Nova Scotia				

### 2.3.2 Ground-based retrievals of AOD

The basic AERONET instrument is the CIMEL sun photometer / sky radiometer manufactured by CIMEL Électronique. Different versions of the CIMEL exist (most notably the version that incorporates two additional NIR / SWIR channels at 1020 nm and 1640 nm and a version that permits nominal AOD sampling time intervals of 3



minutes as opposed to the older standard of 15 minutes). Except for Barrow with a nominal sampling time of 15 minutes, all instruments used in this study were versions incorporating the NIR/SWIR and 3-minute sample time capabilities. Solar extinction measurements acquired by the CIMEL instruments permit the retrieval of AOD spectra across eight channels (340, 380, 440, 550, 670, 870, 1020 and 1640 nm). The SDA is employed by AERONET to produce  $\tau_f$  and  $\tau_c$  estimates at a reference wavelength of 500 nm.

Combined solar extinction and sky radiance measurements are acquired at a significantly lesser (nominal) sampling frequency of once an hour and are employed in an AERONET inversion algorithm to extract columnar estimates of particle size distribution (PSD) and refractive index (Dubovik and King, 2000). The size distribution and refractive index can then be reprocessed to extract estimates of  $\tau_f$  and  $\tau_c$  across the 4 retrieval wavelengths (which can then be extrapolated to, for example, the standard SDA wavelength of 500 nm). The partitioning into  $\tau_f$  and  $\tau_c$  is accomplished by defining a cut-off bin size corresponding to the minimum of the retrieved volume PSD (i.e. a variable cut-off radius). The cut-off radius, the retrieved PSD and the refractive indices are then employed to extract  $\tau_f$  and  $\tau_c$ .

The sampling rate is the key to the usage made of the different types of available retrievals: high frequency event-level studies and comparisons with lidar data are performed using 3-minute AOD spectra separated into  $\tau_f$  and  $\tau_c$  (see for example, Saha et al., 2010) while low frequency, climatological-scale analyses are carried out using the more comprehensive Dubovik inversions to extract  $\tau_f$  and  $\tau_c$ . While some comparisons have been made between the SDA and Dubovik retrievals of  $\tau_f$  and  $\tau_c$  (see O'Neill et al., 2003) the Dubovik retrievals are much more of a climatological-scale standard than the SDA retrievals. We accordingly chose to use the Dubovik retrievals of  $\tau_f$  and  $\tau_c$  for the climatological-scale comparisons employed in this paper. The SDA retrievals were employed to investigate / identify specific events that were suspected of being artifactual in nature (statistical outlier events).

### 2.3.3 Level 1.5 versus Level 2.0 retrievals

Dubovik retrievals are available at Level 1.5 and Level 2 processing levels. The quality assurance criteria that define each level are given in Holben et al. (2006). In general, Level 1.5 retrievals are subject to certain QA protocols such as scan symmetry checks and requirements that (Level 2.0 extinction mode) AODs be acquired near the time of the almucantar scan (Level 2.0 extinction – mode AODs are defined at [http://aeronet.gsfc.nasa.gov/new\\_web/data\\_description\\_AOD\\_V2.html](http://aeronet.gsfc.nasa.gov/new_web/data_description_AOD_V2.html)). The scan symmetry criteria along with the requirement for nearby Level 2.0 extinction-mode AODs amount to a form of cloud screening that is arguably more demanding than the extinction-mode AOD cloud-screening criteria that is incorporated in the Level 2.0 extinction-mode product. Level 2.0 retrievals are subject to additional QA criteria such as a maximum allowable sky radiance retrieval error (i.e. error residuals between the computed and measured almucantar sky radiance) and a minimal solar zenith angle.

Table 2 compares Level 1.5 and Level 2.0 statistics for the three AOD components ( $\tau_a$ ,  $\tau_f$ ,  $\tau_c$  at 500 nm) and the ensemble of all five Arctic sites across the 2009 - 2012 MYSP employed in this paper. In terms of total numbers, there are about a factor of 3 ½ times more Level 1.5 measurements than Level 2.0 measurements (5739 versus 1670). While Level 2.0 retrievals are the recommended option for users of AERONET retrieval products, we chose to use Level 1.5 retrievals because of the significantly greater number of points and the expected benefit of greater statistical robustness. At the same time, we monitored the Level 1.5 and Level 2.0 products at every averaging level in order to better understand any significant differences.

Table 2. Ensemble monthly means of Level 1.5 and Level 2.0 AOD components and the differences of two levels for 5 Arctic stations over the period of 2009-2012.

Month	Level 1.5			Level 2.0			$\langle \tau_x \rangle_{2.0} - \langle \tau_x \rangle_{1.5}$				
	$N_k$	$\langle \tau_f \rangle$	$\langle \tau_c \rangle$	$\langle \tau_a \rangle$	$N_k$	$\langle \tau_f \rangle$	$\langle \tau_c \rangle$	$\langle \tau_a \rangle$	$\Delta \langle \tau_f \rangle$	$\Delta \langle \tau_c \rangle$	$\Delta \langle \tau_a \rangle$
March	83	0.068	0.0113	0.0793	19	0.0553	0.0032	0.0585	-0.0127	-0.0081	-0.0207
April	532	0.0811	0.0135	0.0946	231	0.0768	0.01	0.0868	-0.0043	-0.0035	-0.0078
May	1154	0.0814	0.0111	0.0925	666	0.0783	0.0088	0.0872	-0.0031	-0.0022	-0.0053
June	1494	0.0711	0.0037	0.0748	353	0.0795	0.0047	0.0843	0.0084	0.0011	0.0095
July	1277	0.0787	0.0021	0.0808	178	0.0903	0.0029	0.0933	0.0116	0.0008	0.0124
August	921	0.0615	0.0021	0.0636	113	0.0584	0.0021	0.0605	-0.0031	0.0001	-0.0031
September	278	0.0475	0.0023	0.0498	110	0.0543	0.0013	0.0555	0.0068	-0.0011	0.0057
Year	5739	0.0731	0.0055	0.0786	1670	0.0764	0.0065	0.0829	0.0034	0.0010	0.0043

With respect to Table 2, the most notable differences occur in the months of March, June and July with values of  $\langle \tau_{a,2.0} \rangle - \langle \tau_{a,1.5} \rangle = -.021$ , 0.010 and 0.012 respectively and an average of  $-0.003$  for the rest of the months (numbers that can be contextualized by corresponding Level 1.5 standard deviations of 0.041, 0.065, and 0.059). The month of March has only 83 and 19 measurements respectively across the Level 1.5 and 2.0 ensembles: in such cases of near marginal statistics associated with very low numbers of retrievals (always problematic during the Polar dusk months of March and September), our feeling is that Level 2.0 measurements are much more likely to be subject to the vagaries of unrepresentative measurements than Level 1.5 data. The ensemble statistics for the months of June and July are subject to large  $\tau_f$  variations (the standard deviations are large for both Level 1.5 and Level 2.0 data): this is likely due to seasonal smoke events (see the station by station fine mode discussion below).

### 2.3.4 GEOS-Chem simulations

The model that we employed for our comparisons was Version 9-01-03 of the GEOS-Chem global chemical transport model (GC). It is driven by GEOS-5 assimilated meteorological fields from the NASA Goddard Modelling and Assimilation Office (GMAO). We used a 15-minute time step for transport and a 60-minute time step for chemistry and emissions, a latitude / longitude grid size of  $2^\circ$  by  $2.5^\circ$  (approximately 220 km x 50 km at the high Arctic latitude of 0PAL and PEARL and 220 km x 90 km at

Barrow) 47 vertical levels up to 0.01 hPa. The temporal resolution of the GC AODs which we employed in our analysis was 6 hours.

An overview of AOD physics and chemistry in GC is given in Park et al., (2004). We divided the simulated AODs into their fine and coarse mode components ( $\tau_{f,GC}$  and  $\tau_{c,GC}$ ) using the species by species segregation provided by GC. The species are fine mode organic carbon (OC), sulfate (SO<sub>4</sub>) and black carbon (BC) along with fine and coarse mode sea-salt (SS) as well as fine and coarse mode mineral dust). Accordingly;

$$\tau_{c,GC} = \tau_{c,GC,SS} + \tau_{c,GC,dust} \quad (4a)$$

$$\tau_{f,GC} = \tau_{f,GC,SO_4} + \tau_{f,GC,BC} + \tau_{f,GC,OC} + \tau_{f,GC,SS} + \tau_{f,GC,dust} \quad (4b)$$

All AODs are calculated at 550 nm using RH-dependent aerosol optical properties (see Martin et al., 2003 for an overview of the optical processing employed for GC aerosols). The dry-mass particle size distributions of all components except dust are represented by lognormal distributions implicitly partitioned into fine and coarse mode components according to their effective radius ([http://wiki.seas.harvard.edu/geos-chem/index.php/Aerosol\\_optical\\_properties](http://wiki.seas.harvard.edu/geos-chem/index.php/Aerosol_optical_properties)). Dust is represented by a gamma distribution divided into 7 size bins (ibid): in this paper, we defined the fine and coarse mode cut-off radius for dust to be at 1.0  $\mu\text{m}$  (meaning 4 fine-mode bins and 3 coarse-mode bins).

Emission sources in GEOS-Chem are generally dynamic with ties to temporally varying empirical indicators of emission strength (see "Aerosol emissions" on the GEOS-Chem Wiki site at [http://wiki.seas.harvard.edu/geos-chem/index.php/Aerosol\\_emissions](http://wiki.seas.harvard.edu/geos-chem/index.php/Aerosol_emissions)). Biomass burning emissions, for example, employ GFED3 emission estimates which are, in turn, based on MODIS-Terra and MODIS-Aqua fire counts acquired over sampling intervals of 3 hours. As another relevant example, dust emissions are driven dynamically by mobilization schemes that employ analysed wind fields.

### 2.3.5 AOD differences due to small changes in the reference wavelength: GC versus AERONET retrievals

The standard GC optical outputs are at 550 nm while, for reasons of coherency with our

past calculations and those of others, we chose a reference wavelength of 500 nm for the AERONET retrievals. The expected negative bias of the 550 nm AODs relative to 500 nm AODs is generally small compared to the retrieval standard deviations (<~ 20% of the ensemble monthly standard deviations for the fine, coarse and total components)

## 2.4. Results and discussions for the Canadian Arctic

### 2.4.1 Analysis of lognormal versus normal representations

Figure 2 (a) shows normal and lognormal histogram representations of the total AOD ( $\tau_a$ ) for both the AERONET retrievals (Level 1.5) and GEOS-Chem simulations respectively (for all points of the MYSP). In keeping with the conclusions of O'Neill et al. (2000) the top two AERONET histograms confirm that a lognormal representation is more appropriate for Arctic data (the histogram on the logarithmic scale looks more like a normal distribution, while the histogram on the linear scale shows a typical asymmetric, positively skewed, form). The bottom two histograms of Figure 2 (a) illustrate that the GC modelled histograms show the same general characteristics as their measured analogues. This general agreement in the form of measured and modelled histograms (also a characteristic of the fine and coarse modes) is a verification of the real-world simulation capability of the model: an element of model evaluation that we have not noted in the literature.

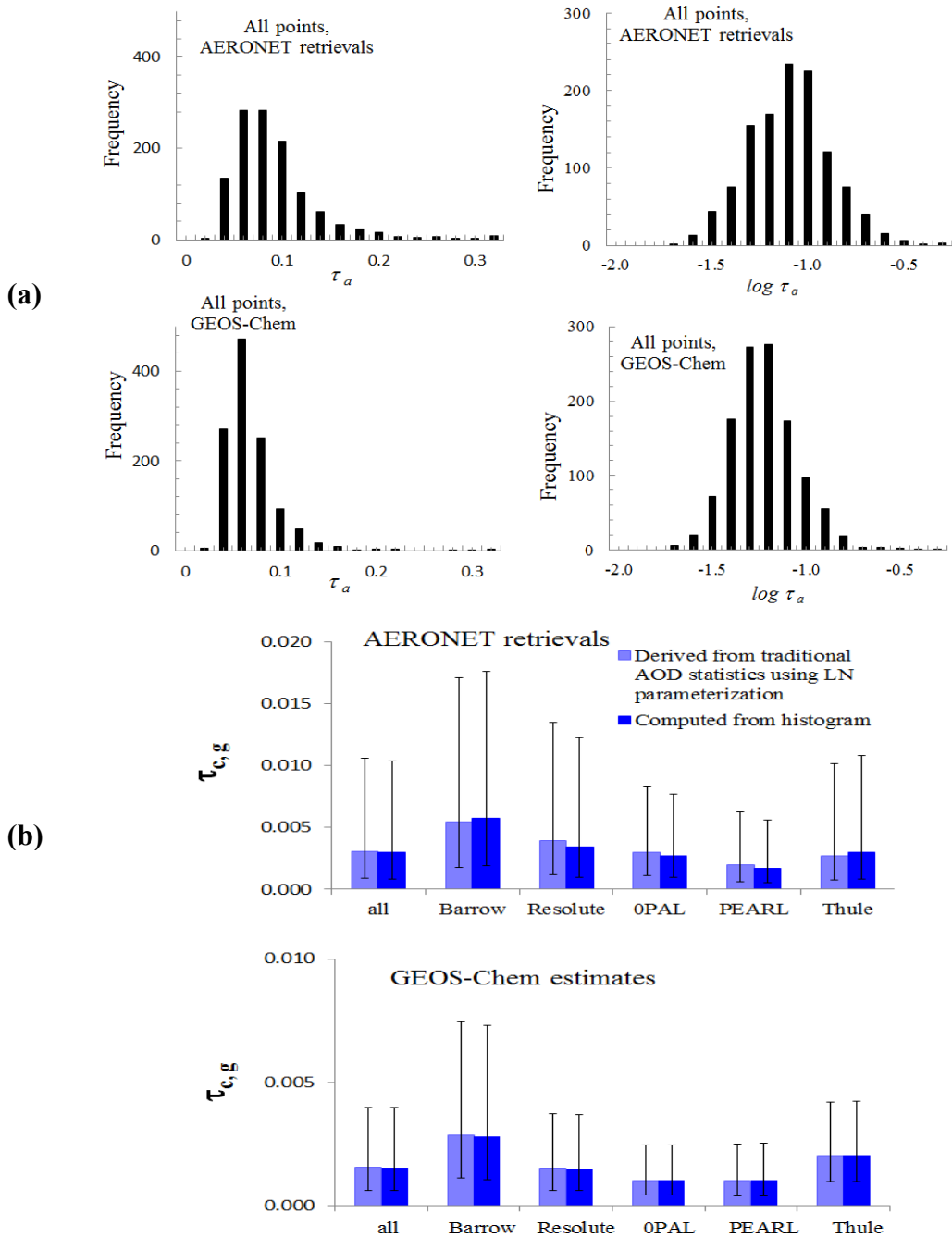


Figure 2. Normal and log-normal fit comparisons for AERONET and GC AOD histograms (a) Linear and lognormal histograms (left and right-hand graphs, respectively) for AERONET at  $\lambda = 500$  nm and GC at  $\lambda = 550$  nm (top and bottom rows respectively), (b) An example of how to employ the traditional means of reporting sun photometry AOD statistics (linear mean and standard deviation) to extract parameters that are representative of the lognormal distribution. In this illustration the linear mean and standard deviation are used to estimate the geometric mean of the histogram by calculating the latter from the lognormal parameterization (equations (2) and (3)).

Figure 2 (b) illustrates the estimation of the geometric mean of an AOD histogram, given the lognormal parameterization and the arithmetic mean statistics (given equation (3)). For this particular coarse mode example (as a function of station for all points during the MYSP) we compare the computed geometric mean from equation (2) with the actual geometric mean of the data histogram for both the AERONET retrievals and GC simulations (the disparity between the optical depth amplitudes of the measured and modelled results will be discussed below). The results show that the geometric mean values from equation (2) are close to the geometric means from the data histograms for both the AERONET retrievals and the GC simulations (less than 20% and 5% difference for measurements and models respectively): this is really just an illustrative confirmation that measured and modelled AOD histograms are better represented by a lognormal distribution. In terms of the overwhelmingly common tendency to report AOD statistics in terms of arithmetic statistics, this result indicates that geometric statistics can be readily retrieved by future analysts and modellers from the arithmetic statistics (providing the arithmetic statistics include at least the arithmetic mean and standard deviation).

#### 2.4.2 General AOD statistics for the retrievals

##### – General considerations

For various reasons, we chose the climatological sampling period (MYSP) of 2009 - 2012 for the analyses presented in this paper. At the same time, we regularly monitored the robustness of the 2009-2012 statistics compared to the statistics of a longer, 2007 - 2012 MYSP. All months with 10 or fewer retrievals for any given station across our MYSP were excluded from the analyses in order to maintain a rudimentary degree of statistical significance and robustness in the worst cases of sparse data (this eliminated the month of March for PEARL, April for OPAL and all of the October retrievals).

Figure 3 shows a sensitivity study that includes a variety of types of 500 nm AOD monthly averages referenced to the (green colored) monthly averages of Tomasi et al. (2015) for the four sites that were in common between our two studies (the Tomasi study is the only recent sun photometry multi-year analysis that includes AERONET stations common to our own). The solid symbols represent monthly averages of daily averaged

retrievals while the open symbols represent monthly averages employing all individual retrievals (without pre-averaging). The open-symbolled curve in purple (and its standard deviation error bars) represents our monthly averaging scheme over our selected MYSP. The comparisons with Tomasi are not identical even when the MYSP and the averaging scheme are identical because they employed AOD retrievals (solar extinction data) for their statistical analysis while our analysis comes from AODs processed through the AERONET Dubovik retrieval. This brings up an interesting predicament: their analysis nominally employs about a factor of five more AODs (and thus is nominally more statistically sound) than our analysis while one could argue, that the retrievals are better filtered than the AODs (both in terms of cloud screening and in terms of the physical soundness of the derived products; see Holben et al., 2006 for a general discussion of Dubovik retrieval filtering).



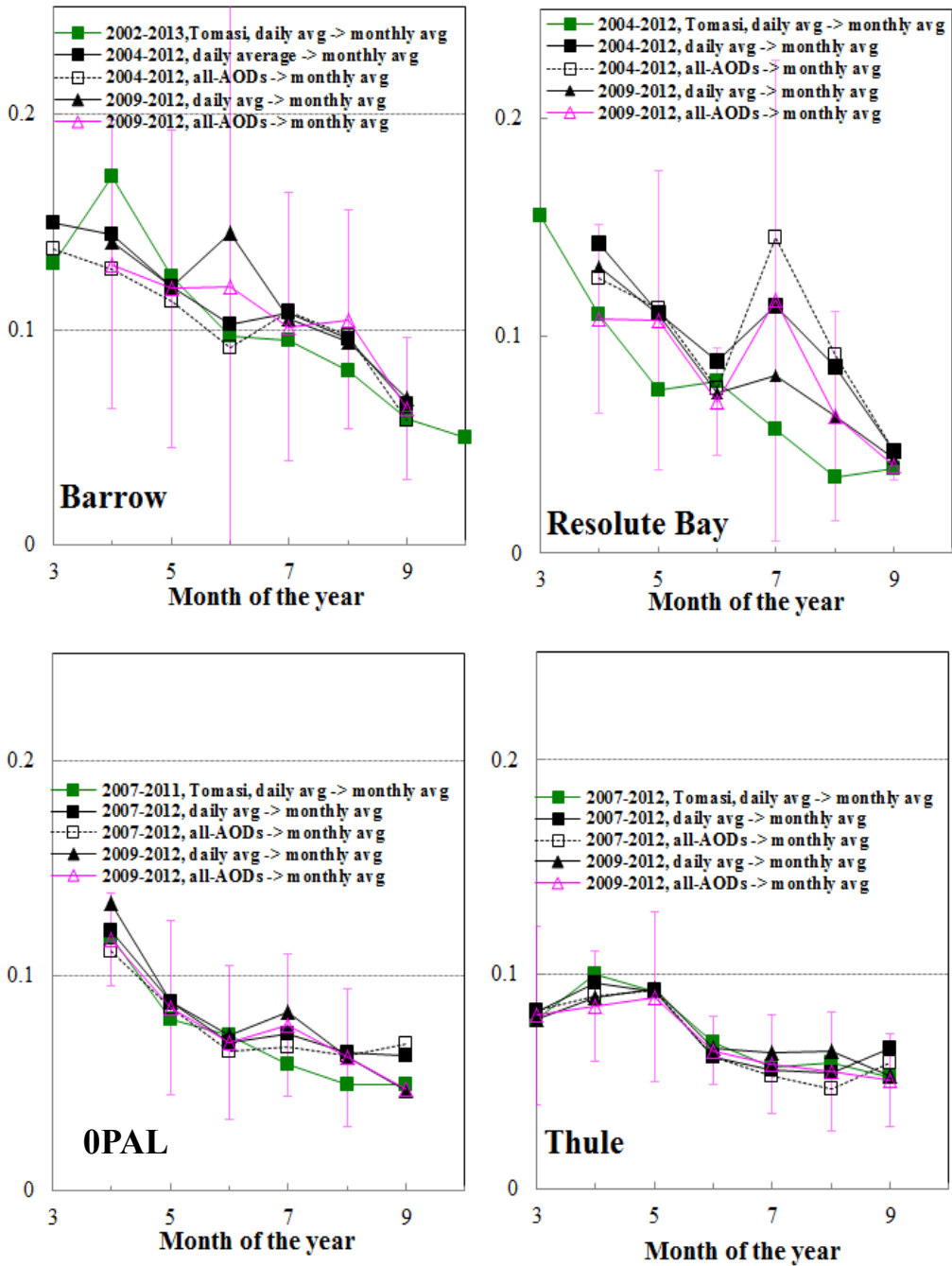


Figure 3. Comparison between various types of monthly averages (black and purple) and the monthly averages (green) of Tomasi et al. (2015). The Tomasi AOD averages represent Level 2.0 extinction data. The purple curve shows the averages for the MYSP. The error bars are standard deviations.

As can be seen in Figure 3, the agreement (of any of the curves) with the station by station, multi-year Arctic AOD analysis of Tomasi (2015) is rather marginal for the two western stations of Barrow and Resolute Bay, affected as they are by intermittent, large-

amplitude smoke events (see the fine mode station by station analysis below for further discussions). Indeed, the results can be rather precarious with large changes between the various types of averaging schemes and with variances that are considerably larger than the eastern station variances (as represented by the standard deviations of our chosen averaging scheme). In one particularly egregious example, the removal of two super-unity  $\tau_f$  days of data from Barrow's "daily avg  $\rightarrow$  monthly avg" scheme for June (black triangles in Figure 3) yielded a reduction in  $\langle \tau_f \rangle$  and  $\sigma(\tau_f)$  of 0.046 and 0.187 respectively for the month of June (in effect the process of daily averaging before monthly averaging enhanced the statistical weight of those two days<sup>2</sup>). This level of precariousness appears to be damped down by averaging over a longer MYSP of 2004 to 2012. However, such was not the case for the highly variable month of July in the Resolute Bay results: the same increase in the MYSP duration produced even greater departures from the Tomasi results. If we leave aside the case of July in Resolute Bay the RMSD values relative to the Tomasi results for our chosen MYSP and all 4 stations (the purple vs the green curves) vary from  $\sim 0.02$  for the western stations to  $\sim 0.01$  for the eastern stations (values that are all  $\sim$  the standard deviations of our chosen MYSP).

#### – Seasonal variations of the total AOD

Figure 4 shows the  $\langle \tau_a \rangle$  monthly mean variation for the total MYSP data ensembles of the 5 Arctic and 10 southern stations (the error bars represent the standard deviations as defined in the section on averaging and standard deviation statistics). In general, one can note the larger (if not always significantly larger) southern AODs and a peaking of the Arctic AODs in April ( $\sim 0.10$ ) with a decrease in the summer to fall period ( $\sim 0.05$  in September) while the southern station ensemble shows AOD (500 nm) peaking during the late summer (c.f. Holben et al., 2000, for general multi-year statistics of southern stations). The 8-station, (1999 - 2011) Arctic (AERONET) averages of Breider et al. (2014) and the (2004 - 2006) Alert results of Hardenberg et al. (2012) show a broadly similar type of (550 nm AOD) behaviour as do the 500 nm results of Tomasi et al.

---

<sup>2</sup> June 12, 13, 2010 for which only 3 Level 1.5 retrievals were actually archived. The "all-AODs $\rightarrow$ monthly averaging" (pink) case placed  $\cong$  a factor of 3 less weight on those 3 measurements for the month of June 2010 (this is reflected in the lower pink triangle in the June, Barrow case of Figure 3).

(2015). Eck et al. (2009) show a similar (500 nm) AOD trend at Barrow for a 1999 - 2008 MYSP (with infrequent, large amplitude excursions due to smoke) while the interior (Boreal forest) Alaskan site of Bonanza Creek showed a smoke dominated peak in August for seasonal statistics across a MYSP of 1994 to 2008.

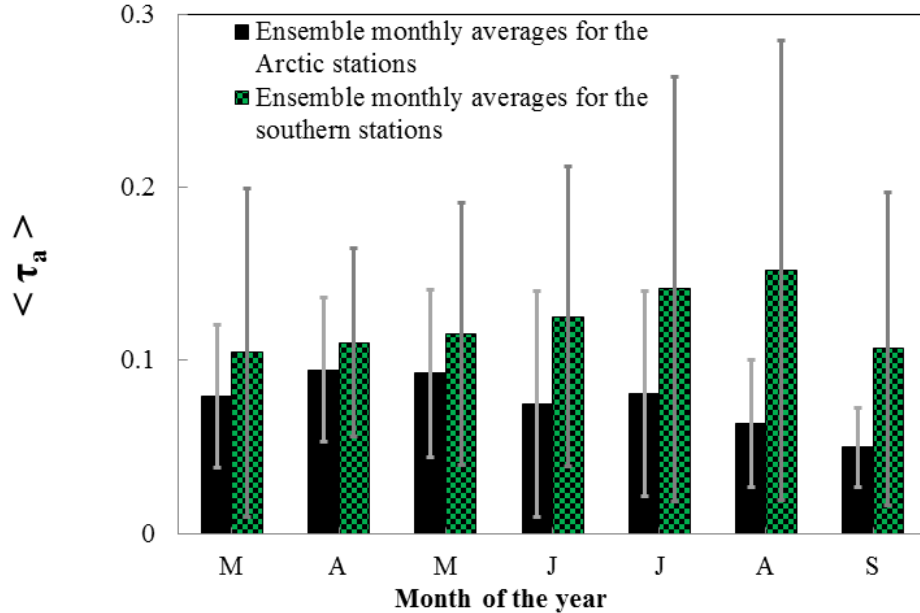


Figure 4.  $\langle \tau_a \rangle$  (averaged over the 2009 to 2112 MYSP) as a function of month for the Arctic stations compared with the analogous averages for the 10 southern stations. The error bars are standard deviations

### 2.4.3 Comparisons with GC

— Component AODs averaged over all stations

Retrieved and modelled seasonal plots of monthly averaged component AODs ( $\langle \tau_f \rangle$ ,  $\langle \tau_c \rangle$  and  $\langle \tau_a \rangle$ ) for all the Arctic stations across our chosen MYSP of 2009 to 2012 are shown in Fig. 5. Both retrieved and modelled plots of  $\langle \tau_f \rangle$  indicate a peak in the April/May period and in July (the latter peaking being not unrelated to the above comparisons with the Tomasi reference). The GC estimations are systematically less than the retrievals but the differences of  $\sim 0.03$  are usually within the retrieval standard deviations.

Peaking of  $\langle \tau_c \rangle$  in April / May can be observed for both the retrievals and GC, with a significant amplitude disparity. GC results are relatively independent of the MYSP while retrieved  $\langle \tau_f \rangle$  and  $\langle \tau_c \rangle$  values are also fairly robust: the RMSD values of  $\langle \tau_f \rangle_{2007-2012}$  —

$\langle \tau_f \rangle_{2009-2012}$  and  $\langle \tau_c \rangle_{2007-2012} - \langle \tau_c \rangle_{2009-2012}$  for the 2007 - 2012 MYSP relative to the 2009 - 2012 MYSP were computed to be 0.0035 and 0.0032 respectively (values that are respectively much smaller than and less than or of the order of the standard deviation error bars seen in Figure 5).

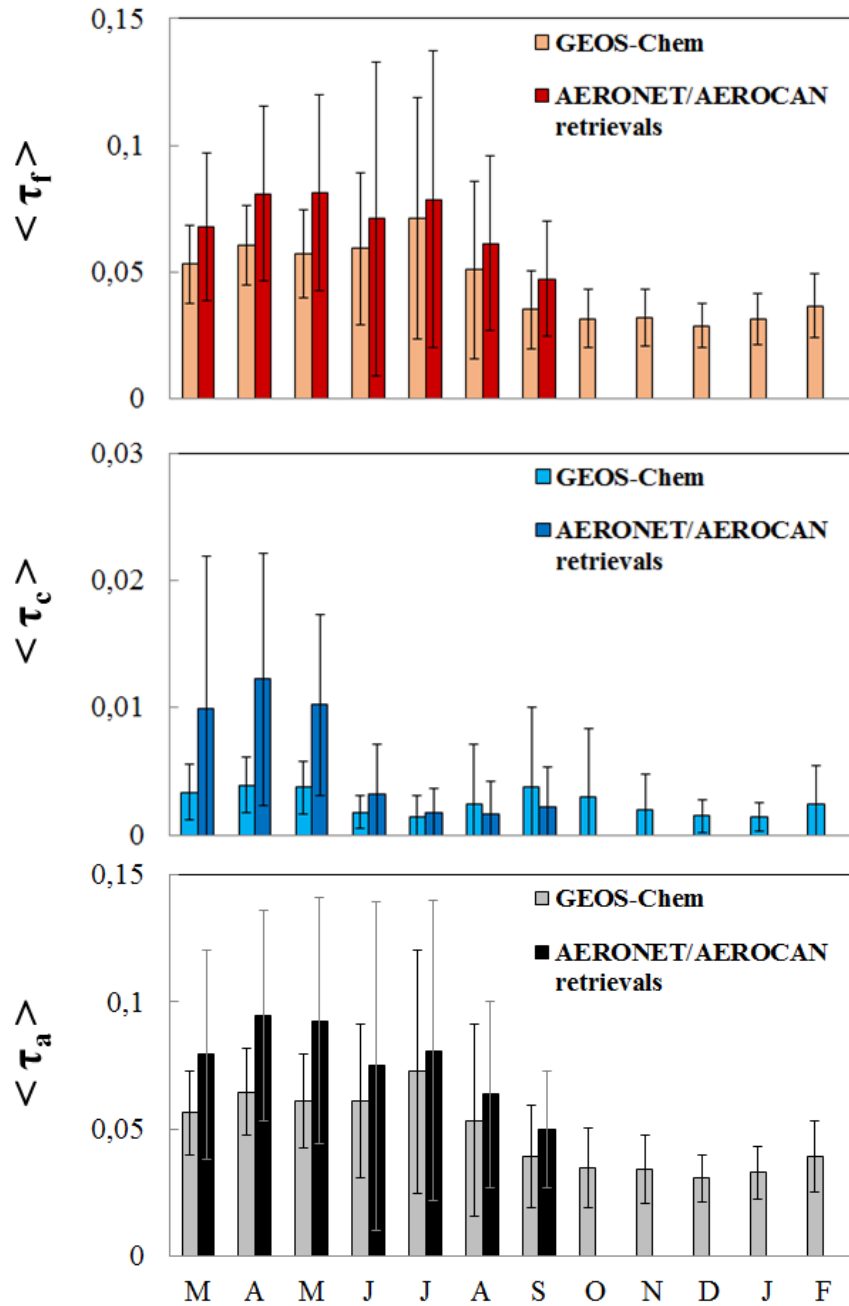


Figure 5.  $\langle \tau_f \rangle$ ,  $\langle \tau_c \rangle$  and  $\langle \tau_a \rangle$  (monthly averages over the 2009 to 2012 MYSP) and modelled values ( $\langle \tau_f, GC \rangle$ ,  $\langle \tau_c, GC \rangle$  and  $\langle \tau_a, GC \rangle$ ) as a function of month. The error bars are standard deviations.

- Individual stations
  - Linear and logarithmic regressions of modelled AOD versus AERONET AODs

Figure 6 shows the GC versus AERONET coefficient of determination ( $R^2$ ) computations for daily averaged  $\tau_a$ ,  $\tau_f$ , and  $\tau_c$  values as a function of the measurement station (as well as the combination of all station data) over the total MYSP. The plot includes a comparison of  $R^2$  for linear regressions (both modelled and AERONET AODs in linear space) as well as logarithmic regressions (both modelled and AERONET AODs in log space). The error bars correspond to one standard deviation of the Fisher's z transformation distribution (see, for example, Siegel, 1961). One can observe that the logarithmic regression is always characterized by a higher  $R^2$  value but that the value is not always significantly higher in the case of  $\tau_f$  and  $\tau_a$  (notably for the eastern Arctic stations). In the case of  $\tau_c$ , the values show a significant improvement over the linear regressions for the "all" (stations) case and for each individual station. A superiority of  $R^2$  values in log-space compared to  $R^2$  values in linear space, for lognormally distributed data frequencies has been noted, for example, by Zerovnik et al. (2013)<sup>3</sup> where the degree of superiority was shown to vary with the strength of correlation between the independent and dependent variables and the COV (coefficient of variation) of the two variables. The results of Figure 6 are, in fact, further confirmation that both the retrieved and modelled AOD distributions are lognormal.

---

<sup>3</sup> Specifically, their Figure 3 where their lognormal coefficient  $C^{(ln)}$  is the coefficient of correlation for the linear space where the data probability distribution appears as lognormal while  $C^{(n)}$  is the coefficient of correlation for the log space where the data probability distribution appears as normal.

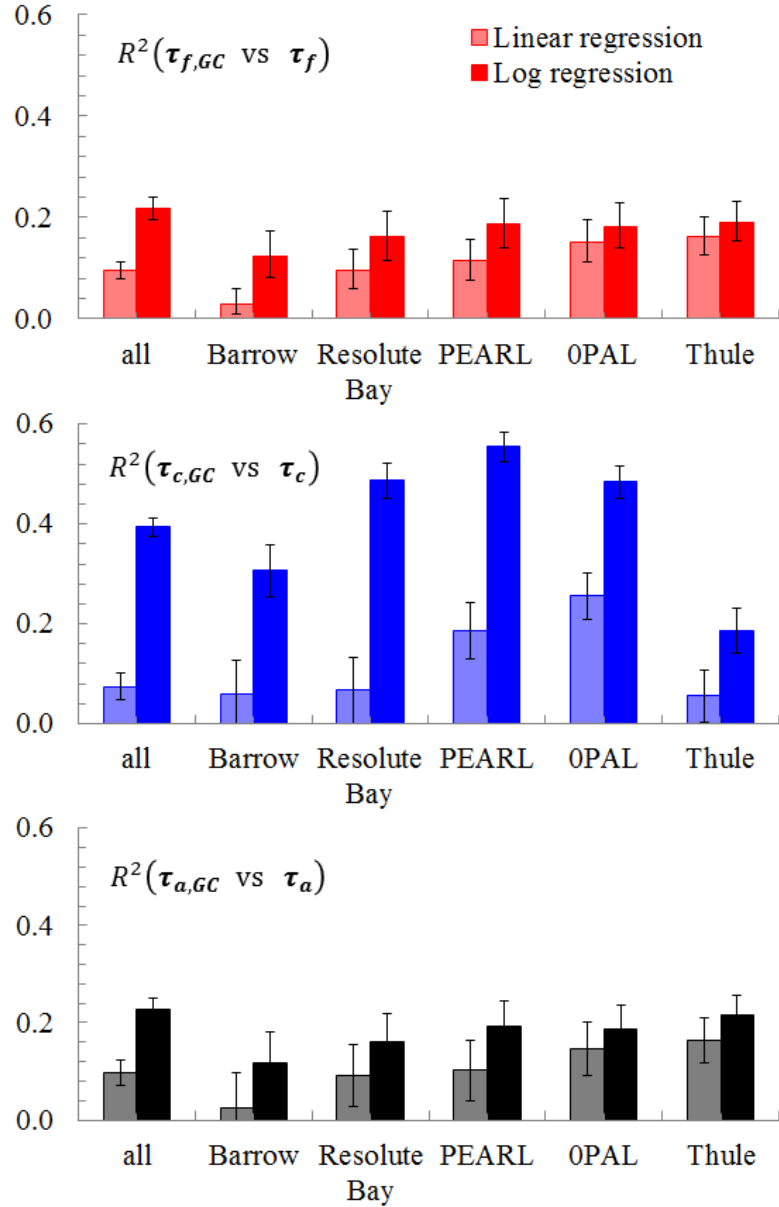


Figure 6. Coefficient of determination between modelled and retrieved daily AOD means for the ensemble of all sites ("all") and for individual sites. The error bars are the standard deviations corresponding to one standard deviation of Fisher's z transformation distribution (see Siegel, 1961, for example).

The superiority of  $R^2$  values in log-space should be at its greatest when the COV is largest (ibid): this is the case for (retrieved and simulated) coarse-mode COVs which were  $>\sim 1$  while fine and coarse-mode COVs were  $<\sim 1$ . The significant logarithmic

correlation is likely an indication that even though  $\langle \tau_c \rangle$  and  $\langle \tau_{c,GC} \rangle$  are  $\ll$  the standard sunphotometer AOD error<sup>4</sup>, their estimation / retrieval significance can be well below that nominal error. This means that the GC estimates can still be physically significant even though, for example, the simulated source strengths might be substantially underestimated. On the retrieval side this means that the estimation of  $\tau_c$  is essentially a small fraction of  $\tau_a$  that depends (mostly) on the spectral shape of the latter: the influence of this spectral shape scales down to the small values of  $\tau_c$  that result from the retrievals.

- Fine mode seasonal variations

Figure 7 shows  $\langle \tau_f \rangle$  and  $\langle \tau_{f,GC} \rangle$  monthly average values for our chosen 2009-2012 MYSP in terms of the individual stations. The first thing we would note is the coherency of the PEARL and OPAL retrievals. The simple average of the monthly average differences ( $\langle \tau_f \rangle_{OPAL} - \langle \tau_f \rangle_{PEARL}$ ) for the OPAL and PEARL bar graphs of Figure 7 is 0.0013: that this is a very small positive number<sup>5</sup> well below the expected errors of CIMEL AODs is fortuitous. However, the fact that it is small in general does permit us to exploit the very useful redundancy afforded by the near co-location of the two instruments.

---

<sup>4</sup> for newly calibrated instruments these are typically  $< 0.01$  for  $\lambda > 440\text{nm}$  and  $< 0.02$  for shorter wavelengths (Holben et al., 1998).

<sup>5</sup> As expected for an OPAL CIMEL instrument which sees a moderately thicker atmosphere from its sea-level location.

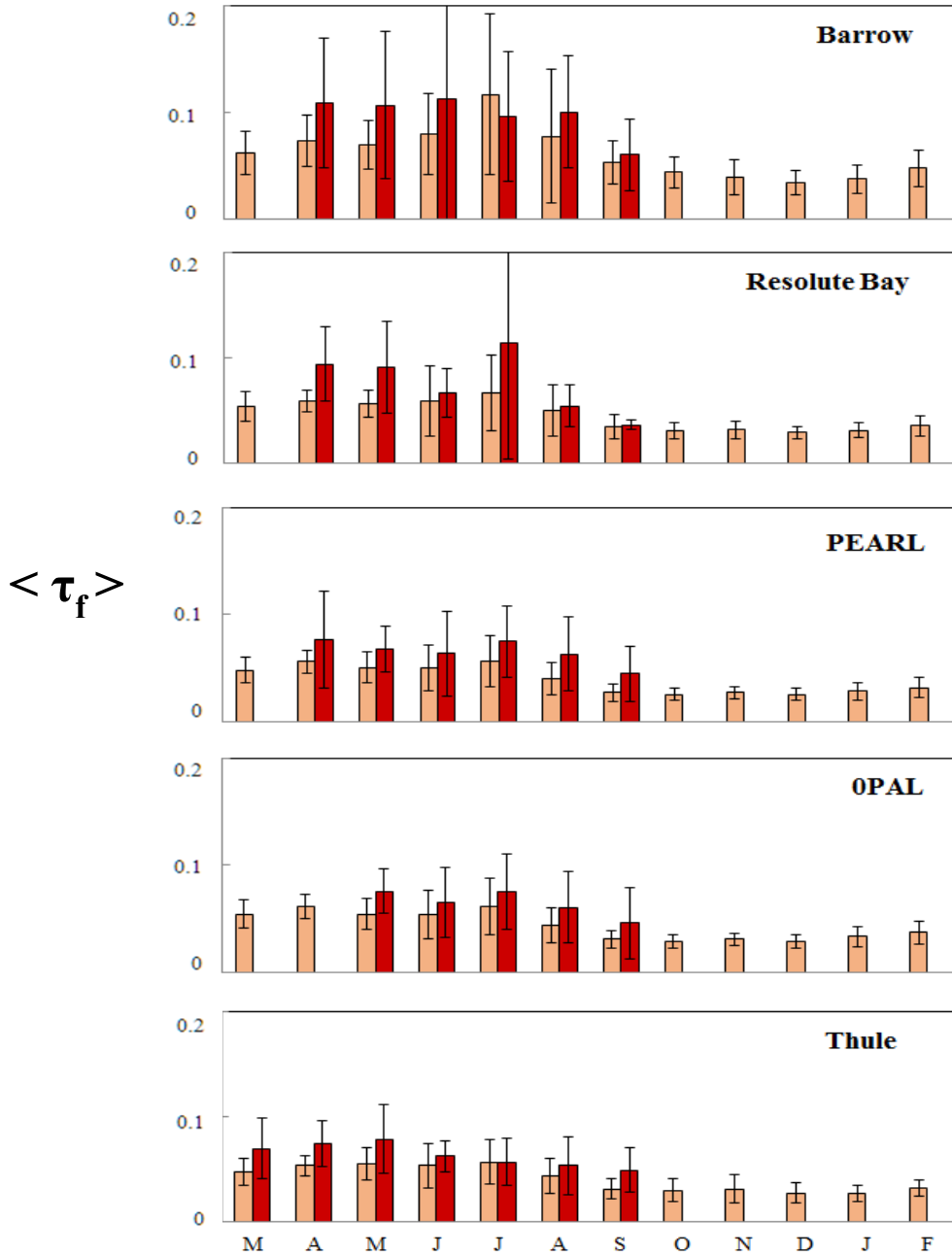


Figure 7.  $\langle \tau_f \rangle$  Fine mode monthly averages over the MYSP for all 5 Arctic sites. The error bars are the standard deviations.

Resolute Bay, as well as OPAL and PEARL to a moderate degree, show  $\langle \tau_f \rangle$  peaking in July while the Resolute Bay standard deviation is very large (COV  $\sim 1.5$ ) in keeping with the general averaging comments made above about the variability of AODs during this month (the fact that both OPAL and PEARL show a weak peak is an example of the



potential values of the redundancy mentioned in the previous paragraph). That this AOD variability is largely in the fine mode and that it is likely smoke, is in keeping with our SDA investigations using individual events during the MYSP and, in general with our SDA / lidar experience that smoke is a common fine mode phenomenon in the Arctic (see Saha et al., 2010 for example). Barrow displays June peaking with a large standard deviation (also in keeping with general averaging comments made above). The fine mode contribution of Resolute Bay is largely responsible for the July peaking seen in Figure 3. That peaking is, at best, marginally evident in the GC simulations and the OC contribution to that marginal peaking is roughly shared between fine mode sea-salt and fine mode sulphates (in other words there is no GC evidence for strong seasonal smoke influence at Resolute Bay during the month of July).

Excluding the peaking of the retrievals in July and the Barrow peak in June (as we did for the Tomasi comparison above and as we noted for the all-station case), one can generally observe a broad and decreasing, spring to fall  $\langle \tau_f \rangle$  trend displayed by all the stations with a peak in April / May. The  $\langle \tau_{f,GC} \rangle$  curves show a broad and weak peak in April / May with a moderate July inflection: this behaviour results from a combination of a strong biomass-burning OC peak in May and a decreasing sulphate trend from an Arctic haze peak in February, both of which decrease until June where they tend to flatten out. The average GC underestimate relative to the retrievals, for all the sites is 0.0132 (a general figure, without excluding any months).

- Coarse mode seasonal variations

Coarse mode,  $\langle \tau_c \rangle$  and  $\langle \tau_{c,GC} \rangle$  monthly average results are shown in Figure 8 for each station. We found infrequent but strong  $\tau_c$  outlier excursions in the individual retrieval results with a significant effect on the monthly means and standard deviations ( $\sim 1$  to  $10$  outlier excursions for  $\sim 20$  to  $400$  retrievals in a given monthly bin over the MYSP). A  $3\sigma$  outlier exclusion filter was accordingly applied to the coarse mode, individual station retrievals and these are the results seen in Figure 8. Investigations of a few trial cases using the SDA applied to high-frequency solar extinction data suggested that these strong  $\tau_c$  excursions were due to temporally and spatially homogeneous clouds whose  $\tau_c$  contributions had not been eliminated by the cloud screening impacts of the Level 1.5

retrieval QA protocols defined in Holben et al. (2006). We note that no appeal could be made to Level 2.0 retrievals since the number of retrievals in a given monthly bin was, more often than not,  $\ll 10$ .

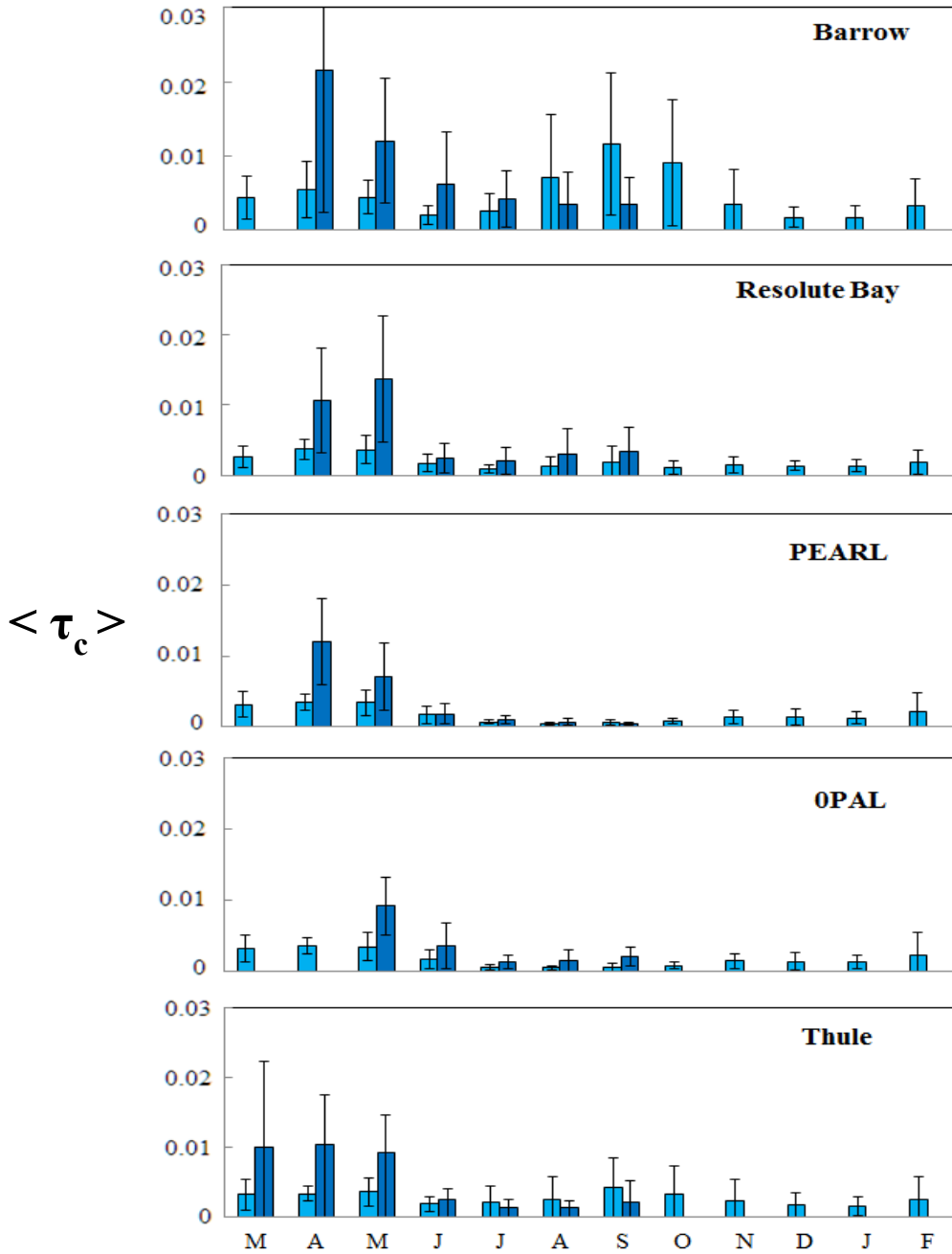


Figure 8.  $\langle \tau_c \rangle$  Coarse mode monthly averages over the MYSP for all 5 Arctic sites. The error bars are the standard deviations.

The AERONET retrievals of Figure 8 indicate  $\langle \tau_c \rangle$  peaking in April / May for all stations while a degree of weak  $\langle \tau_c \rangle$  peaking can be observed in the August /

September period. The  $\langle \tau_{c,GC} \rangle$  simulations show a broad and comparatively weak (dust dominated) peak around the April/May period as well as broad and strong (predominantly sea-salt) peaking at Barrow in the autumn (with comparatively weak dust peaking and / or sea-salt peaking at the other sites). The springtime GC dust simulations are, in fact, predominantly fine mode across all the Arctic stations and across all months with a consistent fraction  $\tau_{f,dust,GC} \sim 2/3$  of  $\tau_{dust,GC}$ . If the AERONET retrievals were similarly affected it would be impossible to subjectively back out such a contribution from the significantly larger  $\tau_f$  values : the coarse mode peak is thus a rather unique optical retrieval indicator of dust and acts somewhat as a dust signature for AERONET retrievals. The fact that the retrievals and GC simulations are in agreement, at least in terms of an April/May peak, lends credence to both the partitioning of the retrieved AOD into fine and coarse modes (where the coarse mode contribution is  $\sim$  typical sun photometry errors) at the same time as it lends credence to the predictive capabilities of GC over the Arctic.

That GC generally tends to underestimate  $\langle \tau_c \rangle$  relative to the retrievals (by up to 75% in the Barrow case for the month of April) while overestimating  $\langle \tau_c \rangle$  in the fall, could certainly be related to the need to better develop GC representation of emissions and atmospheric processes. On a more procedural level the  $\langle \tau_{c,GC} \rangle$  values could be increased in April, for example, by  $\sim 40 - 50\%$  by repartitioning the dust bins to reflect the actual (variable) fine/coarse cut-off radius of AERONET retrievals. However, this only improves the relative agreement with respect to the AERONET retrievals by  $\sim 10 - 15\%$  and degrades the agreement in the fall by  $\sim 10\%$ . The springtime overestimates could also be related to problems in the data and the retrievals; spatially / temporally homogeneous clouds and / or ice crystals are a known issue (O'Neill et al., 2016) and our  $3\sigma$  filtering to eliminate the more egregious instances of this type of problem may well have left residual cloud effects in the coarse mode retrievals (ibid).

In terms of independent support for springtime dust phenomena in the Arctic, numerous authors have reported April / May peaks from climatological-scale in-situ dust measurements (Sirois & Barrie, 1999 at Alert, Fan, 2013 at Alert; Breider, 2014 at Trapper Creek, AK) or from event-based sun photometry supported by back trajectories (Stone et al., 2007 at Barrow). These authors largely attributed the dust presence to Asian

dust (with the exception of Breider et al. (2014) who employed GC simulations to argue for a Saharan dust contribution that was about three times the Asian dust contribution). Empirical evidence for the presence of a fine mode dust component is less common. Brieder et al. (2014) explicitly state that the dust concentration measurements they employed for GC validation at Trapper Creek were fine mode (radius  $< 1.25 \mu\text{m}$ ). We have ourselves, based on more southerly AEROCAN retrievals at Vancouver, BC, suggested the presence of Asian dust which consisted of a mixture of fine and coarse mode particles (Cottle et al., 2013).

## 2.5. Conclusions

We compared GEOS-Chem (GC) simulations of total, fine and coarse mode optical depth ( $\tau_a$ ,  $\tau_f$ , and  $\tau_c$ ) with AERONET retrievals across a four-year sampling period (contextualized by other multi-year sampling periods). We noted that the histograms of both the AERONET retrievals and the GC estimates were better represented by a lognormal distribution (that the statistics were better represented by a geometric mean and geometric standard deviation than an arithmetic mean and standard deviations). Because there is an overwhelming tendency to report AOD statistics in terms of the arithmetic parameters we noted that those parameters could be readily converted to their geometric analogues using analytical, lognormal relationships between the two types of parameters. A marginal  $\log \langle \tau_f \rangle$  correlation and a significant  $\log \langle \tau_c \rangle$  correlation were noted between GC estimates and AERONET retrievals for all the Arctic stations. We noted that logarithmic (log-log or log-space) coefficients of determination for regressions between the model and the retrievals were significantly greater than linear-space correlations, a result that was expected for a lognormal AOD frequency distribution. We further argued that the stronger  $\log \langle \tau_c \rangle$  correlation was related to the premise that the GC estimates and the AERONET retrievals were physically significant, even though  $\langle \tau_{c,GC} \rangle$  values were substantially less than retrievals values and even though the retrieval values were less than or  $\sim$  typical AOD errors.

Our multi-year analysis of the retrievals yielded seasonal (monthly averaged) AODs whose values could be sensitive to how averaging was performed (whether with a different MYSP or a different averaging approach). It was argued that this sensitivity was

largely due to the presence of highly variable  $\tau_f$  values associated with smoke. While distancing the analysis from the problematic months of (respectively), June and July in the Barrow and Resolute Bay data, we found that the station by station seasonal  $\langle\tau_f\rangle$  trend showed a peak in April / May which decreased across the summer period (in other words, since the fine mode generally tends to dominate  $\langle\tau_a\rangle$  we found a trend that is very similar to the  $\langle\tau_a\rangle$  trend: a decrease from a peak  $\sim 0.10$  in April / May to  $\sim 0.05$  in the fall ).

Both the retrievals and GC simulations showed coarse mode seasonal variations with peaks in April / May and August / September. The former are likely due to Asian dust while the latter are, according to the simulations, sea-salt (Barrow) or a weak combination of sea-salt and dust. The GC simulations (and our own measurements of Asian dust in the south) suggest that the April / May dust peaks are characterized by a strong if not dominant fine mode contribution.

The separation of the retrieved AOD into a relatively strong coarse mode component whose presence is also predicted by the GC simulations helps to confirm the general validity and utility of separating AODs into fine and coarse mode components even though the retrieved coarse mode AODs are less than the nominal accuracy of AOD measurements. The separation also provides a coarse mode, optical retrieval "signature" for dust: a fine mode dust contribution (which the GC simulations, in any month at any station, predicted were  $\sim 2/3$  of the dust optical depth) cannot be readily backed out of  $\langle\tau_f\rangle$ . There were large relative differences between the monthly average amplitudes of  $\langle\tau_c\rangle$  and  $\langle\tau_{c,GC}\rangle$ . We argued that this might be model related shortcomings and / or problems with the measurements or the retrievals. In terms of the latter, we found and eliminated rather large excursions in  $\tau_c$  which were likely due to spatially and temporally homogeneous clouds: we tried to eliminate these cases with a  $3\sigma$  outlier but it is difficult to ascertain, in the absence of independent measurements such as lidar profiles whether significant residuals of homogeneous cloud remained.

### **Acknowledgements**

We would like to thank NSERC for CCAR funding via the PAHA and NETCARE projects, the NSERC training program in Arctic Atmosphere Science as well as NSERC DG funding, the CSA, and the CFI for their financial support. The contributions of the

PEARL, AWI and CALIOP operations and processing staff are gratefully acknowledged.

## 2.6. References of the paper

- Barrie, L. A. & Barrie, M. J. (1990) Chemical components of lower tropospheric aerosols in the high Arctic: six years of observations. *Journal of Atmospheric Chemistry*, 11: 211, doi:10.1007/BF00118349.
- Breider, T. J., Mickley, L. J., Jacob, D. J., Wang, Q., Fisher, J. A., Chang, R. Y.-W., & Alexander, B. (2014) Annual distributions and sources of Arctic aerosol components, aerosol optical depth, and aerosol absorption. *Journal of Geophysical Research: Atmospheres*, 119, 4107–4124, doi:10.1002/2013JD020996.
- Cottle, P., Strawbridge, K., McKendry, I., O'Neill, N., & Saha, A. (2013) A pervasive and persistent Asian dust event over North America during spring 2010: lidar and sunphotometer observations. *Journal of Atmospheric Chemistry and Physics*, 13, 4515–4527, doi:10.5194/acp-13-4515.
- Dubovik, O., & King, M. D. (2000) A flexible inversion algorithm for retrieval of aerosol optical properties from Sun and sky radiance measurements. *Journal of Geophysical Research: Atmospheres*, 105, 20,673–20,696, doi:10.1029/2000JD900282.
- Dubovik, O., Smirnov, A., Holben, B.N., King, M. D., Kaufman, Y. J., Eck, T. F., & Slutsker, I. (2000) Accuracy assessments of aerosol optical properties retrieved from Aerosol Robotic Network (AERONET) Sun and sky radiance measurements. *Journal of Geophysical Research*, vol.105(D8), 9791–9806, doi:2000JD900040.
- Eck, T.F., Holben, B.N., Reid, J.S., Sinyuk, A., Hyer, E.J., O'Neill, N.T., ... Newcomb, W. W., (2009) Optical properties of boreal region biomass burning aerosols in central Alaska and seasonal variation of aerosol optical depth at an Arctic coastal site. *Journal of Geophysical Research: Atmospheres*, 114, D11201, doi:10.1029/2008JD010870.
- Eckhardt, S., Quennehen, B., Olivie, D. J. L., Berntsen, T. K., Cherian, R., Christensen, J. H., ... Stohl, A. (2015) Current model capabilities for simulating black carbon and sulfate concentrations in the Arctic atmosphere: a multi-model evaluation using a comprehensive measurement data set. *Journal of Atmospheric Chemistry and Physics*, 15, 9413–9433, doi:10.5194/acp-15-9413.
- Fan, Song-Miao. (2013) Modeling of observed mineral dust aerosols in the arctic and the impact on winter season low-level clouds. *Journal of Geophysical Research: Atmospheres*, 118, 11,161–11,174, doi:10.1002/jgrd.50842.
- Hardenberg, J. von., Vozella, L., Tomasi, C., Vitale, V., Lupi, A., Mazzola, M., ... Provenzale, A. (2012) Aerosol optical depth over the Arctic: a comparison of ECHAM-HAM and TM5 with ground based, satellite and reanalysis data. *Journal of Atmospheric Chemistry and Physics*, 12, 6953–6967, doi:10.5194/acp-12-6953.

- Holben, B. N., Eck, T.F., Slutsker, I., Tanré, D., Buis, J. P., Setzer, A., ... Smirnov, A. (1998) AERONET—A federated instrument network and data archive for aerosol characterization. *Journal of Remote Sensing of Environment*, 66:1–16, doi:10.1016/S0034-4257(98)00031-5.
- Holben, B. N., Tanré, D., Smirnov, A., Eck, T.F., Slutsker, I., Abuhassan, N., ... Zibordi, G. (2001) An emerging ground-based aerosol climatology: Aerosol optical depth from AERONET. *Journal of Geophysical Research: Atmospheres*, 106(D11), pp.12067–12097, doi:10.1029/2001JD900014.
- Holben, B. N., Eck, T. F., Slutsker, I., Smirnov, A., Sinyuk, A., Schafer, J., ... Dubovik, O. (2006) AERONET's Version 2.0 quality assurance criteria. *Proceedings of the SPIE*, vol.6408, id. 64080Q-1, doi:10.1117/12.706524.
- Ignatov, A. & Stowe, L. (2002) Aerosol retrievals from individual AVHRR channels. Part II: Quality control, probability distribution functions, information content, and consistency checks of retrievals. *Journal of the atmospheric sciences*, 59.3, 335-362, doi: 10.1175/1520-0469(2002)059<0335:ARFIAC>2.0.CO;2.
- IPCC: Climate Change 2013: The Physical Science Basis. Contribution of Working Group I to the Fifth Assessment Report of the Intergovernmental Panel on Climate Change [Stocker, T.F., D. Qin, G.-K. Plattner, M. Tignor, S.K. Allen, J. Boschung, A. Nauels, Y. Xia, V. Bex and P.M. Midgley (eds.)], Cambridge University Press, Cambridge, United Kingdom and New York, NY, USA, 1535 pp., 2013.
- Knobelspiesse, K. D., Pietrasa, C., Fargiona, G. S., Wanga, M., Frouine, R., Miller, M. A., ... Balch, W. M. (2004) Maritime aerosol optical thickness measured by handheld sun photometers. *Journal of Remote Sensing of Environment*, 93:1-2, 87–106, doi:10.1016/j.rse.2004.06.018.
- Levy, R. C., Leptoukh, G. G., Kahn, K., Zubko, V., Gopalan, A., & Remer, L. A. (2009) A critical look at deriving monthly aerosol optical depth from satellite data. *IEEE Transactions on Geoscience and Remote Sensing*, vol.47, 2942 – 2956, doi:10.1109/TGRS.2009.2013842.
- Li, S., Garay, M. J., Chen, L., Rees, E., & Liu, Y. (2013) Comparison of GEOS-Chem aerosol optical depth with AERONET and MISR data over the contiguous United States. *Journal of Geophysical Research: Atmospheres*, 118:19, 11,228–11,241, doi:10.1002/jgrd.50867.
- Limpert, E., Stahel, W. A., & Abbt, M. (2001) Log-normal distributions across the sciences: Keys and Clues. *Journal of BioScience*, 51(5):341-352, doi:10.1641/0006568(2001)051[0341: LNDATS]2.0.CO;2.
- Martin, R.V., Jacob, D. J., Yantosca, R. M., Chin, M., & Ginoux, P. (2003) Global and regional decreases in tropospheric oxidants from photochemical effects of aerosols. *Journal of Geophysical Research: Atmospheres*, 108(D3), 4097, doi:10.1029/2002JD002622.
- Matthias, V., Balis, D., Bösenberg, J., Eixmann, R., Larlori, M., Komguem, L. (2004) Vertical aerosol distribution over Europe: Statistical analysis of Raman lidar data from 10

- European Aerosol Research Lidar Network (EARLINET) stations. *Journal of Geophysical Research: Atmospheres*, 109.D18201, doi:10.1029/2004JD004638.
- O'Neill, N. T., Ignatov, A., Holben, B. N., & Eck, T. F. (2000) The lognormal distribution as a reference for reporting aerosol optical depth statistics; empirical tests using multi-year, multi-site AERONET sunphotometer data. *Geophysical Research Letters*, vol.27, I 20, 3333-3336, doi:10.1029/2000GL011581.
- O'Neill, N. T., Eck, T. F., Holben, B. N., Smirnov, A., Dubovik, O., & Royer, A. (2001) Bimodal size distribution influences on the variation of Angstrom derivatives in spectral and optical depth space. *Journal of Geophysical Research: Atmospheres*, 106(D9), 9787-9806, doi:10.1029/2000JD900245.
- O'Neill, N. T., Eck, T. F., Smirnov, A., Holben, B. N., & Thulasiraman, S. (2003) Spectral discrimination of coarse and fine mode optical depth, *Journal of Geophysical Research: Atmospheres*, 108(D17), 4559,4559-4573, doi:10.1029/2002JD002975.
- O'Neill, N. T., Pancrati, O., Baibakov, K., Eloranta, E., Batchelor, R. L., Freemantle, J., ... Lindenmaier, R. (2008) Occurrence of weak, sub-micron, tropospheric aerosol events at high Arctic latitudes. *Geophysical Research Letters*, vol.35, L14814, doi:10.1029/2008GL033733.
- O'Neill, N. T., Baibakov, K., Hesaraki, S., Ivanescu, L., Marrtin, R. V., Perro, C., ... Duck, T.J. (2016) Temporal and spectral cloud screening of polar-winter aerosol optical depth (AOD): impact of homogeneous and inhomogeneous clouds and crystal layers 3 on climatological-scale AODs. *Journal of Atmospheric Chemistry and Physics*, doi:10.5194/acp-2016-296.
- Park, R. J., Jacob, D. J., Field, B. D., Yantosca, R. M., & Chin, M. (2004) Natural and transboundary pollution influences on sulfate-nitrate-ammonium aerosols in the United States: Implications for policy. *Journal of Geophysical Research: Atmospheres*, 109, D15204, doi:10.1029/2003JD004473.
- Perrone, M. R., Santese, M., Tafuro, A. M., Holben, B., & Smirnov, A. (2005) Aerosol load characterization over South-East Italy for one year of AERONET sun-photometer measurements. *Journal of Atmospheric Research*, vol.75, 1-2, 111-133, doi:10.1016/j.atmosres.2004.12.003.
- Saha, A., O'Neill, N. T., Eloranta, E., Stone, R. S., Eck, T. F., Zidane, S., ... McArthur, L. J. B. (2010) Pan-Arctic sunphotometry during the ARCTAS-A campaign of April 2008. *Geophysical Research Letters*, vol.37, L05803, doi:10.1029/2009GL041375.
- Shindell, D. T., Chin, M., Dentener, F., Doherty, R. M., Faluvegi, G., Fiore, A. M., ... Zuber, A. (2008) A multi-model assessment of pollution transport to the Arctic. *Journal of Atmospheric Chemistry and Physics*, 8, 5353-5372, doi:10.5194/acp-8-5353.
- Siegel, M. R., & Stephens, L. J. (1961) *Statistics Fourth Edition*, Schaum's outline series, McGraw-Hill, doi:10.1036/0071485848.
- Sirois, L., & Barrie, L. A. (1999) Arctic lower tropospheric aerosol trends and composition at Alert, Canada: 1980–1995. *Journal of Geophysical Research: Atmospheres*, vol.104(D9), 11599–11618, doi:10.1029/1999JD900077.



- Stone, R. S., Anderson, G. P., Andrews, E., Dutton, E. G., Shettle, E. P., & Berk, A. (2007) Incursions and radiative impact of Asian dust in northern Alaska. *Geophysical Research Letters*, vol.34, L14815, doi:10.1029/2007GL029878.
- Tomasi, C., Kokhanovsky, A. A., Lupi, A., Ritter, C., Smirnov, A., O'Neill, N. T., ... Piketh, S. J. (2015) Aerosol remote sensing in polar regions. *Journal of Earth-Science Reviews*, 140: 108-157, doi: 10.1016/j.earscirev.2014.11.001.
- Twomey, S., & Howell, H. B. (1967) Some aspects of the optical estimation of microstructure in fog and cloud. *Vol.6(12):2125-2131*, doi:10.1364/AO.6.002125.
- Whitby, K. T., Husar, R. B., & Liu, B. Y. H. (1972) The aerosol size distribution of Los Angeles smog. *Journal of Colloid and Interface Science* 39(1):177-204, doi:10.1016/0021-9797(72)90153-1.
- Žerovnik, G., Trkov, A., Smith, D. L., Capote, R. (2013) Transformation of correlation coefficients between normal and lognormal distribution and implications for nuclear applications. *Nuclear Instruments and Methods in Physics Research Section A, Accelerators Spectrometers Detectors and Associated Equipment* 727:33–39, doi: 10.1016/j.nima.2013.06.025.

## Symbol and acronym glossary

AERONET	World-wide NASA network of combined sunphotometer / sky-scanning radiometers manufactured by CIMEL Électronique. See <a href="http://aeronet.gsfc.nasa.gov/">http://aeronet.gsfc.nasa.gov/</a> for documentation and data downloads
AEROCAN	Federated Canadian subnetwork of AERONET run by Environment and Climate Change Canada (ECCC)
AOD	The community uses "AOD" to represent anything from nominal aerosol optical depth which hasn't been cloud-screened to the conceptual (theoretical) interpretation of aerosol optical depth. In this paper we use it in the latter sense and apply adjectives as required.
COV	Coefficient of variation
MYSP	Multi-year sampling Period (spring 2009 to fall 2012) for which we compared AERONET component AODs with GC. Comparisons between the statistics of this MYSP were made
GC	GEOS-Chem, version 9.01.03. <u>FlexAOD</u> (Flexible AOD) is employed to perform offline
$R^2$	Coefficient of determination
SDA	Spectral Deconvolution Algorithm described in O'Neill et al. (2003).
$\tau_x$	$\tau_a$ , $\tau_f$ , or $\tau_c$ for total, fine and coarse mode AODs. Without explicit subscript qualification to GC, this nomenclature is reserved for outputs of the Dubovik retrieval algorithm (at 500 nm). $\tau_f$ , or $\tau_c$ is conserved in the sense that $\tau_a = \tau_f + \tau_c$ . This expression propagates thorough daily and monthly averages.
$\langle \tau_x \rangle$	Arithmetic mean for monthly averaging bins (see the section entitled "Averaging and standard deviation statistics")
$\sigma(\tau_x)$	Arithmetic standard deviation for monthly averaging bins (see the section entitled "Averaging and standard deviation statistics")
$\tau_{x,g}$	Geometric mean for monthly averaging bins. $\tau_{x,g} = 10^{\langle \log \tau_x \rangle}$ (see Table 1 of O'Neill et al., 2000).
$\mu_x$	Geometric standard deviation for monthly averaging bins. $\mu_x = 10^{\sigma(\log \tau_x)}$ (see Table 1 of O'Neill et al., 2000).
$\tau_{x, GC}$	GEOS-Chem estimate of $\tau_x$ at 550 nm.
$x$	$x = a, f, \text{ or } c$ (total, fine mode or coarse mode)

## CHAPTER 3. Conclusions and recommendations

Climatologically (monthly) averaged GEOS-Chem fine, coarse and total AODs ( $\langle\tau_f\rangle$ ,  $\langle\tau_c\rangle$  and  $\langle\tau_a\rangle$ ) were compared with sunphotometer AODs from 5 Arctic measurement sites (Barrow, Resolute Bay, the Eureka sites of PEARL & OPAL and Thule) across a measurement period from Jan.2009 to Jan. 2013. Comparisons were made with 10 southern Canadian stations as a means of better understanding the relative turbidity of the Arctic sites and as a means of investigating the commonalities between the AODs for these distinct regions. Same comparisons were also made for a longer 6-year period from January, 2007 to January, 2013 in order to investigate the robustness of seasonal variations in the retrievals and the model.

In this study, the GEOS-Chem subdivision into fine or coarse mode AODs was based on aerosol types. Dubovik retrievals (level 1.5 and level 2.0) were employed because of their climatological appropriateness (in certain respects, notably because of their inclusion of sky radiance information in addition to solar extinction measurements, they are arguably a better indication of the actual aerosol properties in the atmosphere).

We explored different approaches of formulating monthly statistics in the paper (averages of daily averages, averages of individual retrievals, etc). This statistical approach could result in large variations in the monthly averages and standard deviations (whatever the averaging technique) when large artefactual events occurred at a given station (notably large artefactual fine-mode smoke AODs at Barrow and Resolute Bay (a different, year to year perspective, on the large variations in the months of June and July can be observed in the all-station, fine mode plots of Figure 10 in Appendix B). We also found that the means of characterizing the statistics (log-normal frequency distributions versus normal distributions) was an attribute that was common to both the retrievals and the model. One can refer to the submitted paper (second chapter of the master thesis) for more details on the conclusions of our study.

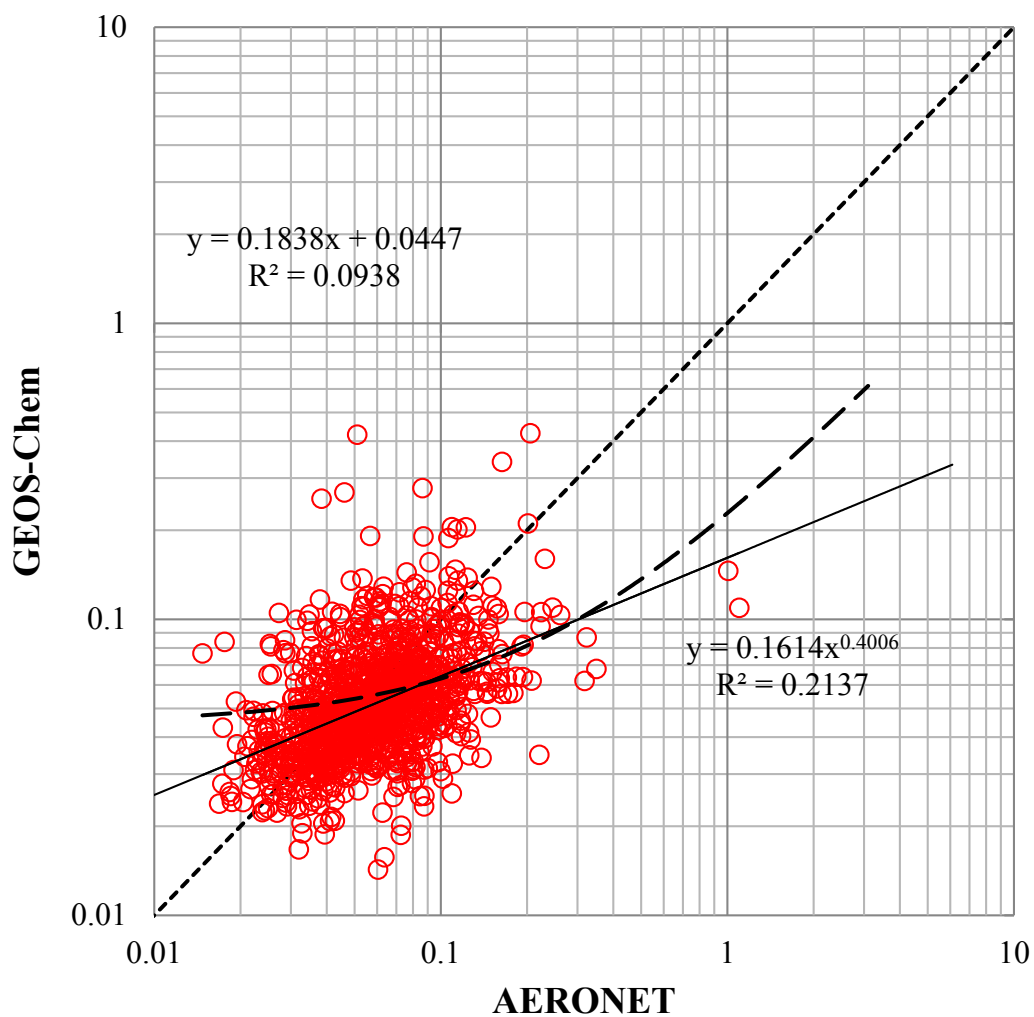
There are a few improvements that can be suggested as recommendations of this study :

- More Arctic stations, especially stations located outside the Canadian Arctic would test the pan-Arctic commonalities and differences of the AOD retrievals and the GEOS-Chem comparisons (but this is a mandate that is outside of the requirements of the NETCARE project).
- We need to extend the purely extensive-parameter GEOS-Chem investigations of this study to include retrieval / model comparisons of intensive parameters whose scale of variability tends to be regional (currently the Ph.D. project of Yasmin Ahmed Samy Aboelfetouh).
- GEOS-Chem version 9.01.03 was employed in this study. Evaluating new versions of the model will enable us to better understand the impact of using different temporal/spatial model resolutions, modified physical processes, inputs, etc.
- Dubovik retrievals are not possible with Polar winter (starphotometer and moonphotometer) data because these instruments do not perform almucantar scans. Therefore, it will continue to be important to compare GEOS-Chem polar winter simulations with AOD retrievals using a method such as the SDA to extract the fine and coarse mode AODs. To a certain extent this has already been done (O'Neill et al., 2016); what was not done, for example, was to investigate the continuity of the total, fine and coarse mode optical depths from the polar winter to the polar summer during the spring and fall. We also need to analyze the newly acquired Polar winter data that was not included in O'Neill et al. (2016) as well as a longer period of Ny Alesund starphotometer data that was not employed in that paper.

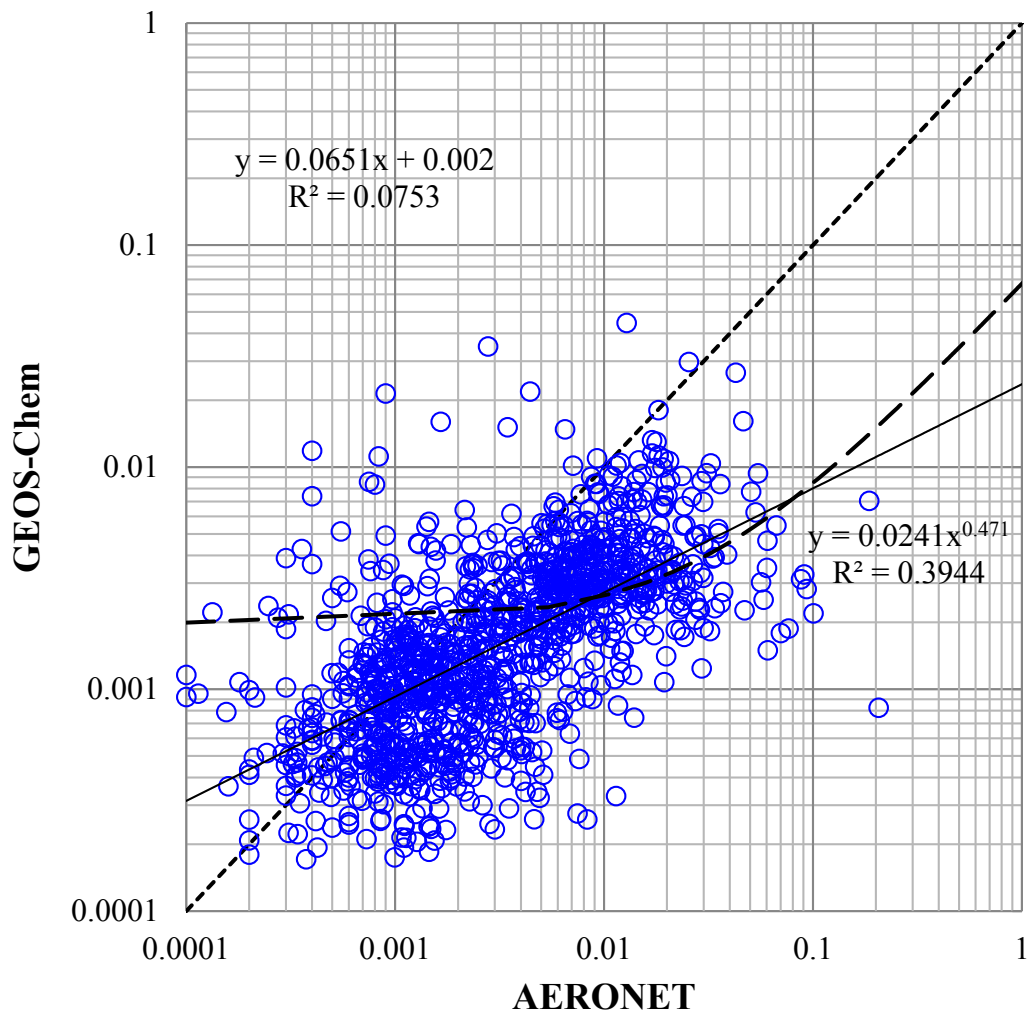
# Appendix A

## Correlation between measurements & model

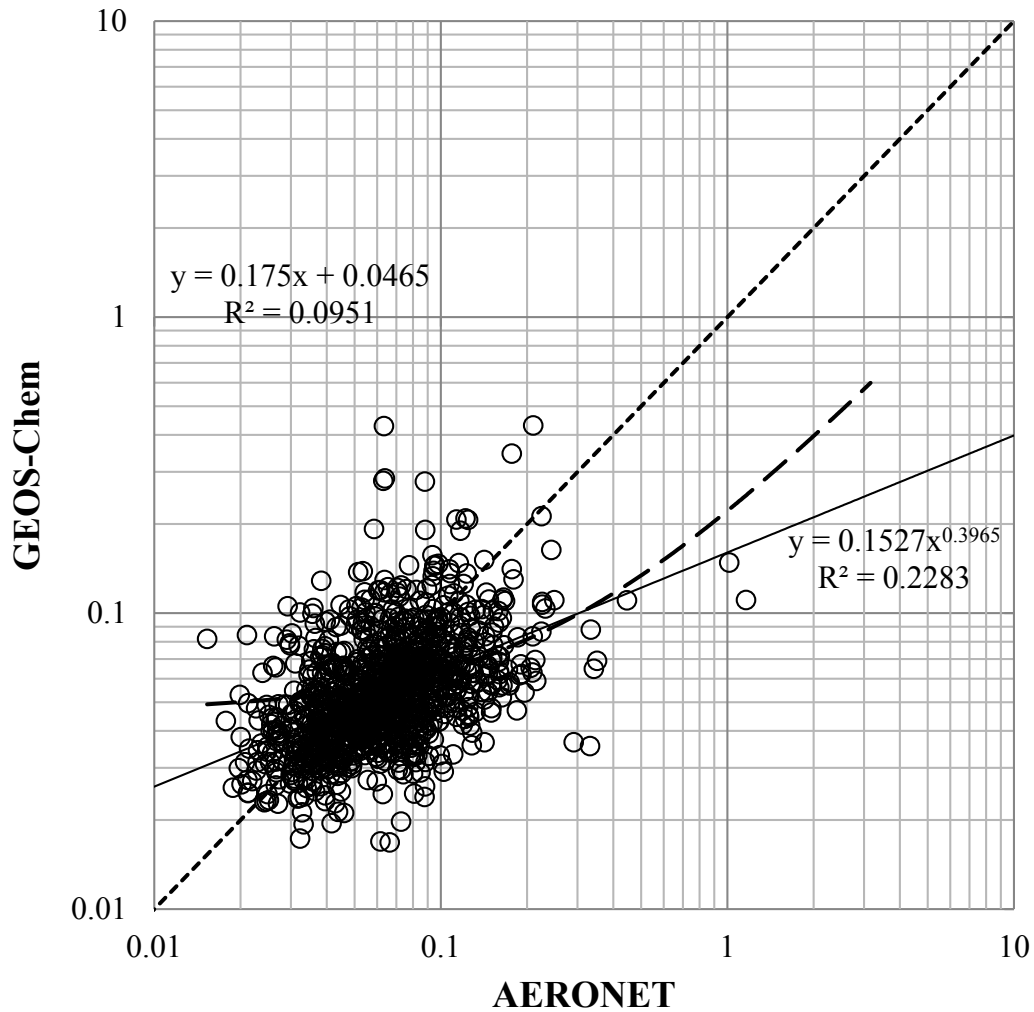
Figure 9 shows the AOD scattergrams between the GEOS-Chem predictions and the AERONET retrievals based on linear and logarithmic regression (in linear-linear and in log-log space respectively). The linear and logarithmic regression equations along with the coefficients of determination ( $R^2$ ) are shown on the top left and bottom right respectively. We have plotted these scattergrams as supplementary data in support of Figure 6 of the submitted article.



(a)



(b)



(c)

Figure 9. Scattergrams in log-log space of the model versus AERONET retrievals (a for file mode, b for coarse mode and c for total AOD) based on a linear regression (bold line) and logarithmic regression (thicker dashed line) for the ensemble of all sites. The very short dashed line is the  $y=x$  line.

## Appendix B

### Intra-annual AODs versus time

Figures 10 and 11 show yearly intra-annual variations of fine and coarse mode AODs over the MYSP for the combined simulations / retrievals of the 5 Arctic stations. We have plotted these intra-annual graphs as supplementary data to provide a different perspective in support of Figures 5, 7 and 8 of the submitted article.

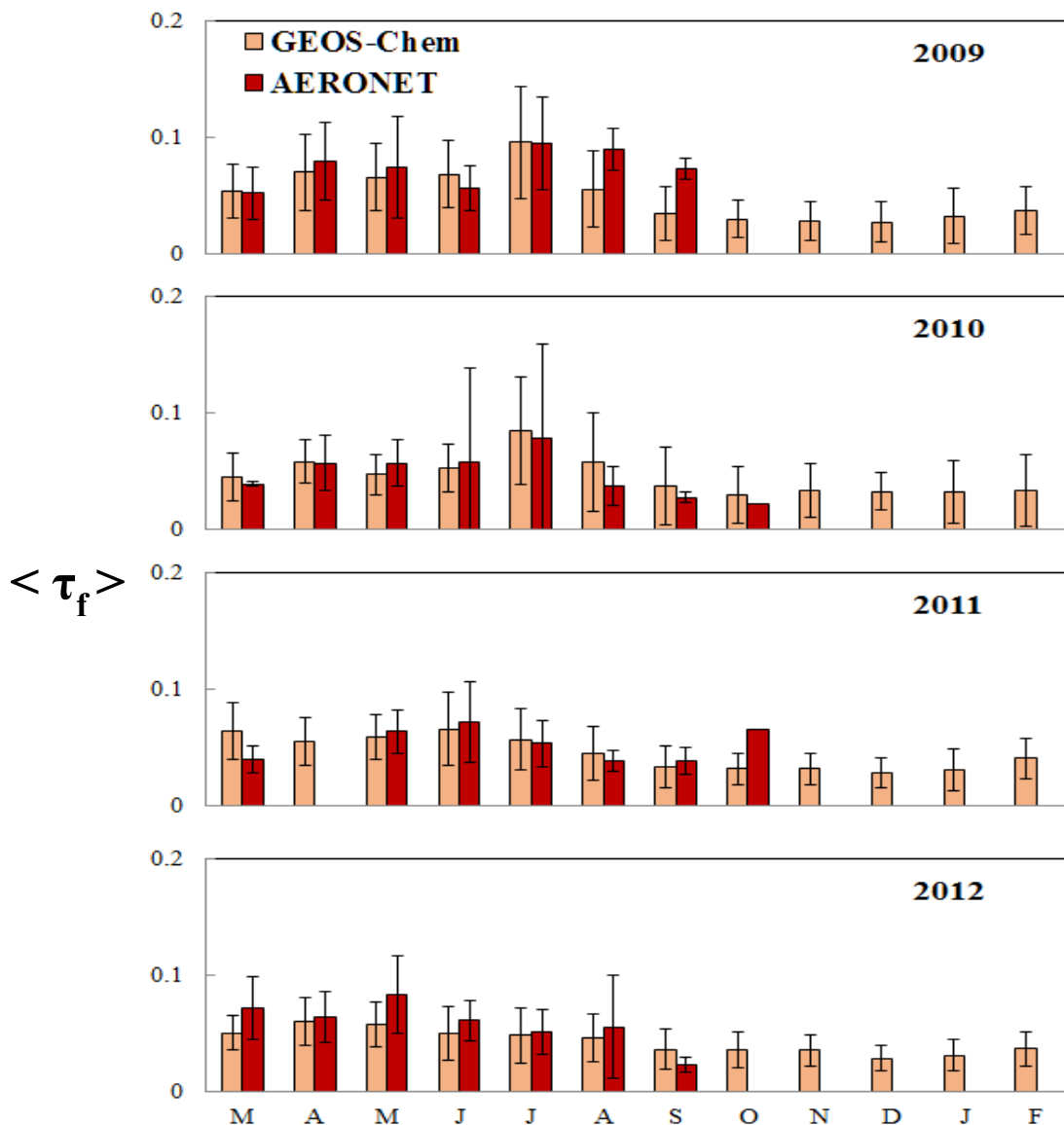


Figure 10. Intra-annual variation of fine AODs over the MYSP



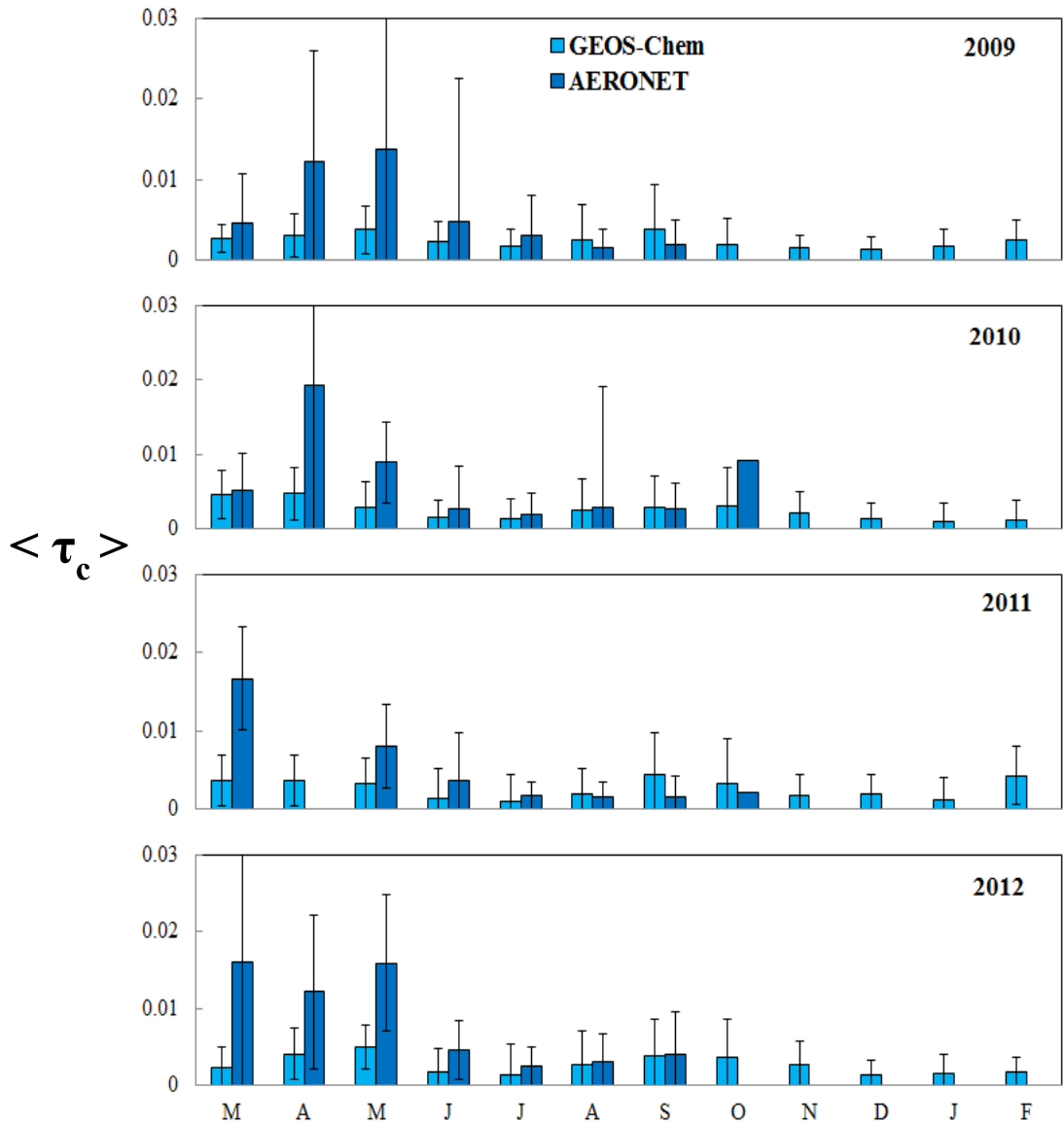


Figure 11. Intra-annual variation of coarse AODs over the MYSP

## References

(Excluding the citations given in SH paper)

- Abbatt, J., NETCARE proposal submitted to NSERC (2012), department of chemistry (st.George campus), University of Toronto.
- Bennouna, Y.S., Cachorro, V.E., Torres, B., Toledano, C., Berjón, A., de Frutos, A.M., and Coppel, I.A.F. (2013), Atmospheric turbidity determined by the annual cycle of the aerosol optical depth over north-center Spain from ground (AERONET) and satellite (MODIS), *Atmospheric Environment*, vol.67, 352-364, doi:10.1016/j.atmosenv.2012.10.065.
- Cheng, T., Gu, X., Xie, D., Li, Z., Yu, T., and Chen, H. (2012), Aerosol optical depth and fine-mode fraction retrieval over East Asia using multi-angular total and polarized remote sensing, *Atmos. Meas. Tech.*, vol.5, 501–516, doi:10.5194/amt-5-501-2012.
- Fairlie, T.D., Jaco, D.J., and Park, R.J., The impact of transpacific transport of mineral dust in the United States (2007), *Atmospheric Environment*, vol.41, 1251–1266, doi: 10.1016/j.atmosenv.2006.09.048.
- Herber, A., Thomason, L.W., Gernandt, H., Leiterer, U., Nagel, D., Schulz, K.-H., Kaptur, J., Albrecht, T., and Notholt, J. (2002), Continuous day and night aerosol optical depth observations in the Arctic between 1991 and 1999, *Journal of Geophysical Research*, vol.107, AAC 6-1–AAC 6-13, doi:10.1029/2001JD000536.
- Hess, M., Koepke, P., and Schult, I. (1998), *Optical Properties of Aerosols and Clouds : The Software Package OPAC*, *journal of American Meteorological Society*, vol.79, doi:10.1175/1520-0477(1998)079<0831:OPOAAC>2.0.CO;2.
- Hinds, W.C., *Aerosol technology, properties, behaviour, and measurement of airborne particles* (1998), 2nd edition, ISBN: 978-0-471-19410-1.
- Husar, R. B., Tratt, D. M., Schichtel, B. A., Falke, S. R., Li, F., Jaffe, D., Gasso', S., Gill, T., Laulainen, N.S., Lu, F., Reheis, M.C., Chun, Y., Westphal, D., Holben, B.N., Gueymard, C., McKendry, I., Kuring, N., Feldman, G.C., McClain, C., Frouin, R.J., Merrill, J., DuBois, D., Vignola, F., Murayama, T., Nickovic, S., Wilson, W.E., Sassen, K., Sugimoto, N., and Malm, W.C. (2001), Asian dust events of April 1998, *Journal of Geophysical Research*, vol.106, 18317-18330, doi:10.1029/2000JD900788.
- Jacob, D. (1999). *Introduction to Atmospheric Chemistry*, pages 144{146. Princeton University Press.
- Martin, M.V., Logan, J.A., Kahn, R.A., Leung, F.Y., Nelson, D.L., and Diner, D.J. (2010), Smoke injection heights from fires in North America : Analysis of 5 years of satellite observations, *Atmos. Chem. Phys.*, vol.10, 1491–1510, doi:10.5194/acp-10-1491-2010.
- Seinfeld, J. H. and Pandis, S. N. : *Atmospheric chemistry and physics : From air pollution to climate change* (2006), 2nd edition, ISBN: 978-0-471-72018-8.
- Van Donkelaar, A., Martin, R.V., Pasch, A.N., Szykman, J.J., Zhang, L., Wang, Y.X. and Chen, D. (2012), Improving the accuracy of daily satellite-derived ground-level fine

aerosol concentration estimates for North America, *Env. Sci. and Tech.*, vol.46, 11971–11978, doi: 10.1021/es3025319.

W.R. Sessions, Reid, J.S., Benedetti, A., Colarco, P.R., Silva, A. da., Lu, S., Sekiyama, T., Tanaka, T.Y., Baldasano, J.M., Basart, S., Brooks, M.E., Eck, T.F., Iredell, M., Hansen, J.A., Jorba, O.C., Juang, H.-M.H., Lynch, P., Morcrette, J.-J., Moorthi, S., Mulcahy, J., Pradhan, Y., Razinger, M., Sampson, C.B., Wang, J., and Westphal, D.L. (2015), Development towards a global operational aerosol consensus : basic climatological characteristics of the International Cooperative for Aerosol Prediction Multi-Model Ensemble (ICAP-MME), *Atmos. Chem. Phys.*, vol.15, 335-362, doi:10.5194/acp-15-335-2015.